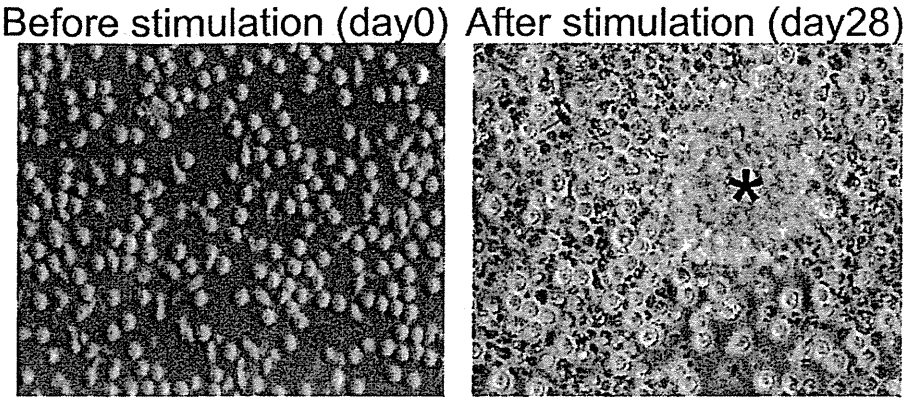

Fig. 4 Morphological change of CTL after stimulation by APC. Before and after stimulation. $CD8^+$ cells make clusters (*asterisk*) in a good culture conditions. Magnification, 400×

Acknowledgements

This study was supported by a Grant-in-Aid for Scientific Research from the Ministry of Education, Culture, Sports, Science and Technology of Japan (to N.S.) program for developing the supporting system for upgrading education and research from the Ministry of Education, Culture, Sports, Science and Technology of Japan (to N.S.) and Takeda Science Foundation (to Y.H.).

References

1. Rosenberg SA et al (2004) Cancer immunotherapy: moving beyond current vaccines. Nat Med 10:909–915
2. Perez SA et al (2010) A new era in anticancer peptide vaccines. Cancer 116:2071–2080
3. Hirohashi Y et al (2009) The functioning antigens: beyond just as the immunological targets. Cancer Sci 100:798–806
4. van der Bruggen P et al (1991) A gene encoding an antigen recognized by cytolytic T lymphocytes on a human melanoma. Science 254:1643–1647
5. Sahin U et al (1995) Human neoplasms elicit multiple specific immune responses in the autologous host. Proc Natl Acad Sci USA 92:11810–11813
6. Rosenberg SA (1999) A new era for cancer immunotherapy based on the genes that encode cancer antigens. Immunity 10:281–287
7. Polyak K, Riggins GJ (2001) Gene discovery using the serial analysis of gene expression technique: implications for cancer research. J Clin Oncol 19:2948–2958
8. Parker KC et al (1994) Scheme for ranking potential HLA-A2 binding peptides based on independent binding of individual peptide side-chains. J Immunol 152:163–175
9. Lin HH et al (2008) Evaluation of MHC class I peptide binding prediction servers: applications for vaccine research. BMC Immunol 9:8
10. Hirohashi Y et al (2002) An HLA-A24-restricted cytotoxic T lymphocyte epitope of a tumor-associated protein, survivin. Clin Cancer Res 8:1731–1739
11. Hariu H et al (2005) Aberrant expression and potency as a cancer immunotherapy target of inhibitor of apoptosis protein family: livin/ML-IAP in lung cancer. Clin Cancer Res 11:1000–1009
12. Inoda S et al (2009) Cep55/c10orf3, a tumor antigen derived from a centrosome residing protein in breast carcinoma. J Immunother 32:474–485
13. Maeda A et al (2001) Identification of human antitumor cytotoxic T lymphocytes epitopes of

recoverin, a cancer-associated retinopathy antigen, possibly related with a better prognosis in a paraneoplastic syndrome. Eur J Immunol 31:563–572
14. Morrison J et al (1992) Identification of the nonamer peptide from influenza A matrix protein and the role of pockets of HLA-A2 in its recognition by cytotoxic T lymphocytes. Eur J Immunol 22:903–907
15. Koup RA et al (1991) Limiting dilution analysis of cytotoxic T lymphocytes to human immunodeficiency virus gag antigens in infected persons: in vitro quantitation of effector cell populations with p17 and p24 specificities. J Exp Med 174:1593–1600
16. Lee SP et al (1997) Conserved CTL epitopes within EBV latent membrane protein 2: a potential target for CTL-based tumor therapy. J Immunol 158:3325–3334
17. Andersen MH et al (1999) An assay for peptide binding to HLA-Cw*0102. Tissue Antigens 54:185–190

J Cancer Res Clin Oncol (2014) 140:503–513
DOI 10.1007/s00432-014-1593-7

ORIGINAL PAPER

Hypoxia-inducible factor (HIF)-independent expression mechanism and novel function of HIF prolyl hydroxylase-3 in renal cell carcinoma

Toshiaki Tanaka · Toshihiko Torigoe · Yoshihiko Hirohashi · Eiji Sato · Ichiya Honma · Hiroshi Kitamura · Naoya Masumori · Taiji Tsukamoto · Noriyuki Sato

Received: 11 October 2013 / Accepted: 20 January 2014 / Published online: 30 January 2014

Abstract
Purpose We previously found that hypoxia-inducible factor (HIF) prolyl hydroxylase-3 (PHD3) was frequently overexpressed in renal cell carcinomas (RCCs), unlike in normal tissues, and therefore, we studied the mechanism and role of PHD3 expression in RCC.
Methods The von Hippel–Lindau (VHL)-gene-mutant RCC cell lines SMKT-R2 and SMKT-R3 and wild-type VHL cell lines Caki-1 and ACHN were used. Associations of the expression of PHD3 with HIF-α proteins and signal transduction pathways were evaluated under normoxic conditions. The effect of PHD3 on cell proliferation was also examined by small interference RNA and cDNA transfection. Moreover, the prognostic impact of PHD3 expression in clear cell RCC (CCRCC) was evaluated using primary cancer tissues.
Results In SMKT-R2 and SMKT-R3, HIF-α proteins were expressed and PHD3 was highly expressed. On the other hand, ACHN had low expression of HIF-α proteins and PHD3. However, Caki-1 had high expression of PHD3 even though there was no distinct expression of HIF-α proteins. PHD3 expression was inhibited by blockade of Akt and mammalian target of rapamycin (mTOR), but not by HIF-1α and HIF-2α double knockdown. In addition, PHD3 knockdown resulted in the promotion of cell proliferation in SMKT-R2, SMKT-R3 and Caki-1. On the other hand, forced expression of PHD3 reduced cell proliferation in ACHN. In immunohistochemistry, PHD3 expression was a significant factor for better recurrence-free survival in patients with CCRCC.
Conclusions PHD3 expression can be induced by the phosphatidylinositol-3 kinase/Akt/mTOR pathway in RCC independently of HIF proteins. Furthermore, PHD3 has an antiproliferative function independent of HIF protein status in RCC, indicating a novel expression mechanism and function of PHD3.

Keywords HIFPH3 · EGLN3 · Hypoxia-inducible factor · VHL · Renal cell carcinoma · HIF prolyl hydroxylase · Signal transduction

Introduction

Hypoxia-inducible factors (HIFs) are key regulators of the cellular stress response under hypoxic conditions. Under hypoxia, these transcriptional factors induce the expression of more than 60 target genes such as vascular endothelial growth factor (VEGF) and erythropoietin that play roles in tumor progression and contribute to tumor aggressiveness (Maynard and Ohh 2007). The expression of HIF-1α is induced by the activation of several cell signaling pathways. The phosphatidylinositol-3 kinase (PI3K)/Akt signaling pathway can increase the mRNA expression and protein accumulation of HIF-1α (Blancher et al. 2001; Brugarolas et al. 2003; Hudson et al. 2002; Laughner et al. 2001; Pore et al. 2006; Zhong et al. 1998). This pathway acts both through mammalian target of rapamycin (mTOR) and otherwise (Blancher et al. 2001; Hudson et al. 2002;

T. Tanaka · T. Torigoe · Y. Hirohashi · N. Sato
1st Department of Pathology, Sapporo Medical University School of Medicine, South-1, West-17, Chuo-ku, Sapporo 060-8556, Japan

T. Tanaka (✉) · E. Sato · I. Honma · H. Kitamura · N. Masumori · T. Tsukamoto
Department of Urology, Sapporo Medical University School of Medicine, South-1, West-16, Chuo-ku, Sapporo 060-8543, Japan
e-mail: zappa@pop12.odn.ne.jp

Pore et al. 2006; Zhong et al. 1998). On the other hand, HIFs are continuously expressed in cells, but immediately degraded via the proteasomal pathway after ubiquitination under normoxia (Huang et al. 2002). The von Hippel–Lindau (VHL) protein acts as a particle recognition protein of the responsible E3 ubiquitin–ligase complex if two distinct prolyl residues in the oxygen-dependent degradation domain of HIFs are hydroxylated (Bruick and McKnight 2001; Cockman et al. 2000; Ivan et al. 2001; Jaakkola et al. 2001; Yu et al. 2001). This site-specific hydroxylation is catalyzed by hypoxia-inducible factor prolyl hydroxylase domain (PHD), dioxygenases that depend on O_2 and the cosubstrates 2-oxoglutarate and Fe(II) (Hirsila et al. 2003). Three different PHDs, PHD1, PHD2 and PHD3 have been identified. Of them, PHD2 is indispensable for hydroxylation and subsequent degradation of HIF-1α (Berra et al. 2003). However, the differences of their in vivo roles have not been fully clarified. Some studies have pointed out that PHD3 is strikingly induced transiently by hypoxia and displays high substrate specificity. PHD3 may hydroxylate divergent substrates and/or connect divergent cellular responses with HIF (Appelhoff et al. 2004). The hypoxic induction of PHD3 is mediated by accumulation of HIF proteins (del Peso et al. 2003; Marxsen et al. 2004), and a hypoxia-responsive element and HIF-binding site were also identified in the promoter region of the PHD3 gene (Pescador et al. 2005).

PHD3 is barely expressed at the mRNA level in normal tissue other than cardiac and neural tissues, unlike PHD2, which shows mRNA expression ubiquitously in various tissues (Cioffi et al. 2003; Hirsila et al. 2003; Lieb et al. 2002). In previous studies, we found that PHD3 was frequently overexpressed in renal cell carcinomas (RCCs) and demonstrated its usefulness as a novel tumor antigen for immunotherapy and a serological marker for RCC (Sato et al. 2008; Tanaka et al. 2011).

Clear cell renal cell carcinoma (CCRCC), a major type of RCC, is associated with VHL gene inactivation, i.e., point mutation and methylation, in which HIF proteins are not degraded and accumulate (Aprelikova et al. 2004; Maxwell et al. 1999; Shinojima et al. 2007). This may account for the high prevalence of PHD3 expression in RCC (Aprelikova et al. 2004; Marxsen et al. 2004). However, RCC without correlation with VHL inactivation, such as papillary RCC, also shows PHD3 expression (Sato et al. 2008). Although tissue hypoxia may lead to PHD3 overexpression, it is rarely expressed in normal organs, unlike PHD2, another subtype of PHD, which is broadly expressed in various normal organs. Considering this, a specific role of PHD3 in RCC is suggested, but is still unknown. Here, we studied the mechanism and role of PHD3 expression in RCC using RCC cell lines with and without VHL gene mutation, as well as RCC tissues.

Materials and methods

Cell culture and reagents

RCC cell lines SMKT R2 and SMKT R3 were established in our laboratory. Caki-1 and ACHN were purchased from the American Type Culture Collection. All these cell lines were cultured in RPMI 1640 (Sigma-Aldrich) supplemented with 10 % fetal bovine serum (Filtron). Caki-1 was incubated for 24 h with 50 μM LY294002 (Sigma-Aldrich) and 10 nM rapamycin (Cell Signaling Technology) for 24 h, respectively.

Reverse transcriptase polymerase chain reaction (RT-PCR) analysis

Total RNA was isolated from cultured cells using an RNeasy Mini Kit (Qiagen). A cDNA mixture was synthesized from 2 μg of total RNA by reverse transcription using SuperScript III and oligo(dT) primer (Invitrogen Life Technologies) according to the manufacturer's protocol. PCR amplification was done in 50 μL of PCR mixture containing 1 μL of cDNA mixture, 1 μL of KOD Plus DNA polymerase (Toyobo) and 15 pmol primers. The PCR mixture was initially incubated at 94 °C for 2 min followed by 35 cycles of denaturation at 94 °C for 15 s, annealing at 64 °C (for PHD3) or 60 °C (for HIF-1α and HIF-2α) for 30 s and extension at 72 °C for 30 s. The primer pairs 5′-CATCCCTGTCTTGTGTGTGG-3′ (forward) and 5′-CCAACAGCCCTGGATTAAGA-3′ (reverse), 5′-CACAGAAATGGCCTTGTGAA-3′ (forward) and 5′-CCAAGCAGGTCATAGGTGGT-3′ (reverse), and 5′-CAGAGGCCGTACTGTCAACC-3′ (forward) and 5′-ACTTCATGTCCATGCTGTGG-3′ (reverse) were employed for specific detection of PHD3, HIF-1α and HIF-2α, respectively. The expected sizes of the PCR products for PHD3, HIF-1α and HIF-2α were 420, 214 and 227 bp, respectively. For semiquantitative analysis, PCR amplification was done in 20 μL of PCR mixture containing 0.25 μL of the cDNA mixture, 0.1 μL of Taq DNA polymerase (Qiagen) and 12 pmol of primers. The PCR mixture was initially incubated at 94 °C for 2 min, followed by 35 cycles of denaturation at 94 °C for 15 s, annealing at 60 °C for 30 s and extension at 72 °C for 30 s. The sequences of the primer pair for semiquantitative detection of PHD3 were 5′-AATTGCCCTGGAGTACATCG-3′ (forward) and 5′-ACTTCGTGTGGGTTCCTACG-3′ (reverse). The expected size of the PCR product was 555 bp. As an internal control, glyceraldehyde 3-phosphate dehydrogenase expression was detected by using forward primer 5′-ACCACAGTCCATGCCATCAC-3′ and reverse primer 5′-TCCACCACCCTGTTGCTGTA-3′ with an expected PCR product of 452 bp. The PCR products were visualized

with ethidium bromide staining under UV light following electrophoresis on 1.0 % agarose gel.

VHL gene sequencing

Genomic DNA was purified from cultured cells using a QIAamp DNA mini kit (Qiagen). PCR amplification was done as described previously with annealing at 60 °C. Exon 1 was divided in two parts and amplified with the primer pairs, 5′-AGCGCGTTCCATCCTCTAC-3′ and 5′-GGCCTCCATCTCCTCCTC-3′, and 5′-TACGGCCC TGAAGAAGACG-3′ and 5′-GCTTCAGACCGTGCTA TCGT-3′. Exons 2 and 3 were amplified with the primer pairs, 5′-TCCCAAAGTGCTGGGATTAC-3′ and 5′-ATC CTGTACTTACCACAACAACC-3′, and 5′-GCAAAGCC TCTTGTTCGTTC-3′ and 5′-CCATCAAAAGCTGAGAT GAAAC-3′, respectively. The PCR products were visualized as described previously. The specific bands were excised under UV light, and DNA was recovered with a QIAEX II gel extraction kit (Qiagen). The nucleotide sequences of the PCR products were confirmed by direct sequencing using an ABI PRISM 310 Genetic Analyzer and an AmpliCycle sequencing kit (Perkin-Elmer, Foster City, CA).

Immunoblot analysis

Cells were lysed with ice-cold Nonidet P-40 buffer for 60 min as described previously (Yamamoto et al. 2005). The lysates were mixed with 2× sample buffer and boiled for 5 min. Then, they were separated by sodium dodecyl sulfate–polyacrylamide gel electrophoresis (SDS–PAGE) on 7.5 % gels and transferred to polyvinylidene fluoride membranes (Millipore, Billerica, MA, USA). The membranes were blocked with TBS containing 5 % nonfat dried milk. Proteins were detected using a mouse anti-HIF-1α monoclonal antibody (54, 1:500 dilution; BD Transduction Laboratories), mouse anti-HIF-2α monoclonal antibody (ep190b, 1:500 dilution; Novus Biologicals), rabbit anti-Akt monoclonal antibody (C67E7, 1:1,000 dilution; Cell Signaling Tech.), rabbit anti-phospho-Akt (Ser 473) monoclonal antibody (D9E, 1:1,000 dilution; Cell Signaling Tech.), rabbit anti-mTOR polyclonal antibody (1:1,000 dilution; Cell Signaling Tech.), rabbit anti-phospho-mTOR (Ser 2448) polyclonal antibody (1:1,000 dilution; Cell Signaling Tech.) and mouse anti-β-actin monoclonal antibody (AC-15, 1:1,000 dilution; Sigma-Aldrich). The membranes were then stained with a peroxidase-labeled secondary antibody and visualized using an enhanced chemiluminescence detection system (Amersham Life Science, Arlington Heights, IL, USA).

Gene silencing by RNA interference

Small interference RNAs (siRNAs) termed "Stealth RNAs," targeting PHD3 (HSS132640, HSS132641 and HSS132642), HIF-1α (HSS104774, HSS104775 and HSS179231) and HIF-2α (HSS103261, HSS176568 and HSS176569), were purchased from Invitrogen. Negative control siRNAs were purchased from Invitrogen. At 30–50 % confluence, cells of SMKT-R2, SMKT-R3 and Caki-1 in six-well plates were transfected with siRNA duplexes at a final concentration of 33.3 nM, using Lipofectamine RNAiMax (Invitrogen) following the manufacturer's protocol.

Construction of PHD3 plasmid and transient gene transfection

Full-length PHD3 cDNA was amplified from cDNA of RCC cell line SMKT-R3 with PCR using KOD plus DNA polymerase (Toyobo). The primer pair was 5′-CGGGG-TACCATGCCCCTGGGACACATCATG-3′ as a forward primer and 5′-CCGCTCGAGGTCTTCAGTGAGGGCA-GATTC-3′ as a reverse primer (underlines indicate KpnI and XhoI recognition sites, respectively). The PCR product was inserted into the pcDNA3.1 vector (Invitrogen). The cDNA sequence was confirmed by direct sequencing as described above. ACHN cells cultured in 24-well plates were transfected with 0.3 μg of the empty vector or expression vector in 24-well plates, using Fugene HD (Roche) reagent according to the manufacturer's protocol.

Cell proliferation assay

Cell proliferation was determined by counting the cell number. Cells cultured in 24-well plates were collected and stained with 0.4 % trypan blue for 5 min at room temperature. Then, viable cells were determined by trypan blue exclusion and counted using a hematocytometer.

Flow cytometry

Three days after siRNA transfection, the cells were harvested and washed with PBS, followed by fixation with 70 % ethanol overnight at −20 °C. After washing with PBS, the cells were resuspended in PBS containing 250 μg/mL RNase A (Sigma-Aldrich) for 30 min at 37 °C and stained with 50 μg/mL propidium iodide (PI) (Invitrogen) for 10 min at 4 °C in the dark. To calculate the percentage of cells in the G0/G1 phase, S phase and G2/M phase, the results were analyzed by flow cytometry (FACSCalibur, Becton–Dickinson, Franklin Lakes, NJ) with CellQuest and ModFit software analysis.

Patients and tissue samples

We reviewed the clinical pathology archives of 116 patients with CCRCC who underwent radical nephrectomy and partial nephrectomy between 2001 and 2009. We classified clinical stage according to the AJCC classification (Edge et al. 2010). Fuhrman classification was used to assess nuclear grade (Fuhrman et al. 1982). Patients whose tumors contained a sarcomatoid component were excluded.

Immunohistochemistry

Sections (4–5 μm thick) of formalin fixed, paraffin embedded tumors were deparaffinized in xylene and rehydrated in graded alcohol. Antigen retrieval was done by boiling sections for 20 min in a microwave oven in preheated 0.01 mol/L sodium citrate (pH 6.0). Endogenous peroxidase activity was blocked by 3 % hydrogen peroxide in ethanol for 10 min. After blocking with 1 % nonfat dry milk in PBS (pH 7.4), the sections were reacted with the following antibodies. To detect PHD3, a rabbit polyclonal anti-human PHD3 antibody (ab30782, Abcam; diluted 1:200) was used as the primary antibody. Negative controls had the primary antibody replaced by buffer. After standard washing steps, slides were subsequently incubated with a biotinylated secondary antibody and streptavidin–biotin complex (Nichirei), followed by incubation with 3,3′-diaminobenzidine used as the chromogen and counterstaining with hematoxylin. All specimens were reviewed independently using light microscopy in at least five areas at ×400 magnification by pathologists who were blinded to clinicopathological data (TTo and YH). Nuclear or cytoplasmic staining was considered positive.

Statistical analysis

All experiments were independently performed three times in triplicate. Results were given as means SEM. Comparisons between two groups were performed using Student's *t* test, whereas comparisons among multiple groups were done using repeated measures ANOVA. Cause-specific survival (CSS) and recurrence-free survival (RFS) were assessed by the Kaplan–Meier method, and differences between two groups were compared using the log-rank test. Associations of PHD3 expression and clinicopathological features with PFS were evaluated using Cox proportional hazards regression models and summarized with the hazard ratio and 95 % confidence interval.

A value of $p < 0.05$ was considered to indicate statistical significance. The calculations were performed using Statview 5.0 (SAS Institute, Cary, NC).

Results

High expression of PHD3 was observed in VHL-mutant cell lines and in the VHL-wild-type cell line Caki-1

VHL gene sequencing revealed that SMKT-R2 and SMKT-R3 had insertion of thymine between nucleotides #713 and #714 in exon 3 and mutation of guanine to adenine at nucleotide #423 in exon 2, respectively. On the other hand, neither Caki-1 nor ACTH had any mutation in the VHL gene. PHD3 was highly expressed in SMKT-R2, SMKT-R3 and Caki-1 at the mRNA level under normoxia, whereas ACHN had sparse PHD3 expression (Fig. 1a). To evaluate the expression of HIF-1α and HIF-2α at the protein level, Western blot analysis was performed. In SMKT-R2 and SMKT-R3, HIF-1α and HIF-2α proteins were expressed, but they were not distinct in Caki-1 and ACHN (Fig. 1b). PI3K/Akt status was evaluated by Western blot analysis (Fig. 1c). SMKT-R2 and Caki-1 had higher expression of phospho-Akt, whereas SMKT-R3 and ACHN had low levels of expression. To evaluate the influence of the PI3K/Akt pathway on PHD3 expression, SMKT-R2 and Caki-1 were cultured with the PI3K inhibitor LY294002. PHD3 expression was reduced in the presence of LY294002 in Caki-1, but not in SMKT-R2 (Fig. 1d). These results indicated that the PHD3 mRNA expression was highly associated with activation of the PI3K/Akt pathway in the VHL-intact RCC cell lines under normoxic conditions, unlike in the VHL-mutant RCC cell lines, in which the PHD3 expression was more strongly associated with HIF accumulation, probably due to inactive VHL.

Activated PI3K/Akt pathway induced PHD3 mRNA expression in RCC independently of HIF proteins

To verify the HIF-independent mechanism of PHD3 induction, we assessed the expression of PHD3 mRNA in Caki-1 transfected with HIF-1α siRNA and HIF-2α siRNA. Cotransfection of HIF-1α-specific siRNA and HIF-2α-specific siRNA (combinations of HSS104774/HSS103261, HSS104775/HSS103261, and HSS104776/HSS173261) significantly reduced the expression of HIF-1α and HIF-2α compared with control siRNA (Fig. 2a). Double knockdown of HIF-1α and HIF-2α did not affect the expression of PHD3 mRNA (Fig. 2b). In these cells, both LY294002 and rapamycin, an mTOR inhibitor, reduced the expression of PHD3 (Fig. 2c). These results suggested that the expression of PHD3 in RCC was induced by the activated PI3K/Akt/mTOR pathway independently of HIF protein accumulation.

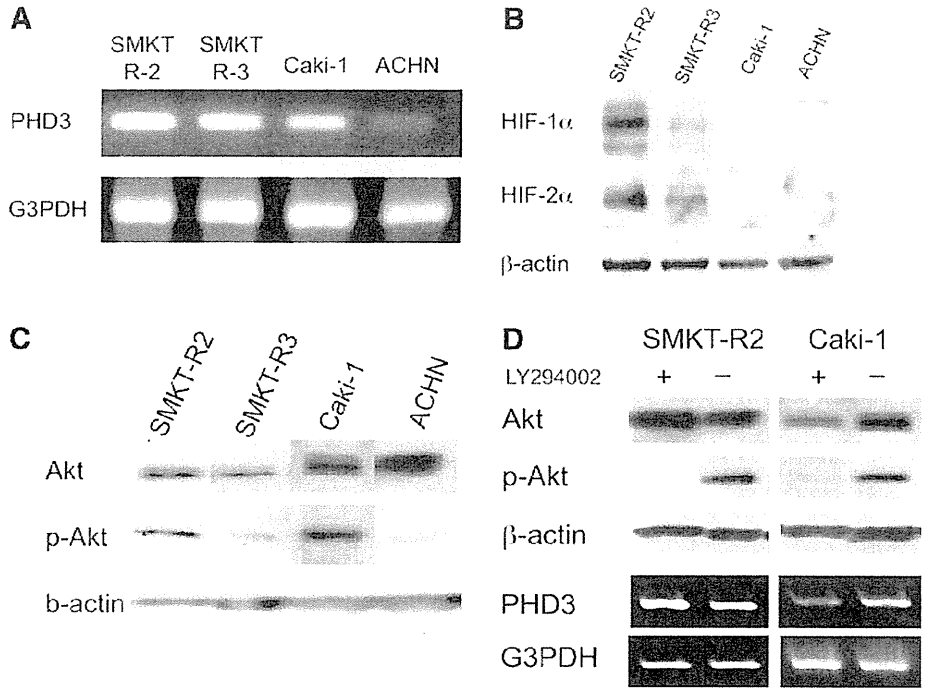

Fig. 1 PHD3 expression in RCC cell lines with and without VHL gene mutation. **a** RT-PCR was performed to evaluate the expression of PHD3. PHD3 was highly expressed in the VHL-mutant cell lines SMKT-R2, SMKT-R3 and VHL-wild-type Caki-1 at the mRNA level under normoxia, whereas ACHN had sparse PHD3 expression. **b** Western blot analysis was performed in cell lines. SMKT-R2 and SMKT-R3 had both HIF-1α and HIF-2α expression, whereas Caki-1 and ACHN had no distinct expression. **c** Caki-1 and ACHN were incubated with 50 μM LY294002 for 24 h, and RT-PCR was performed. The PI3K/Akt pathway was activated and inhibition of PI3K attenuated PHD3 expression in Caki-1, whereas in ACHN, we found neither activation of the PI3K/Akt pathway nor expression of PHD3 mRNA

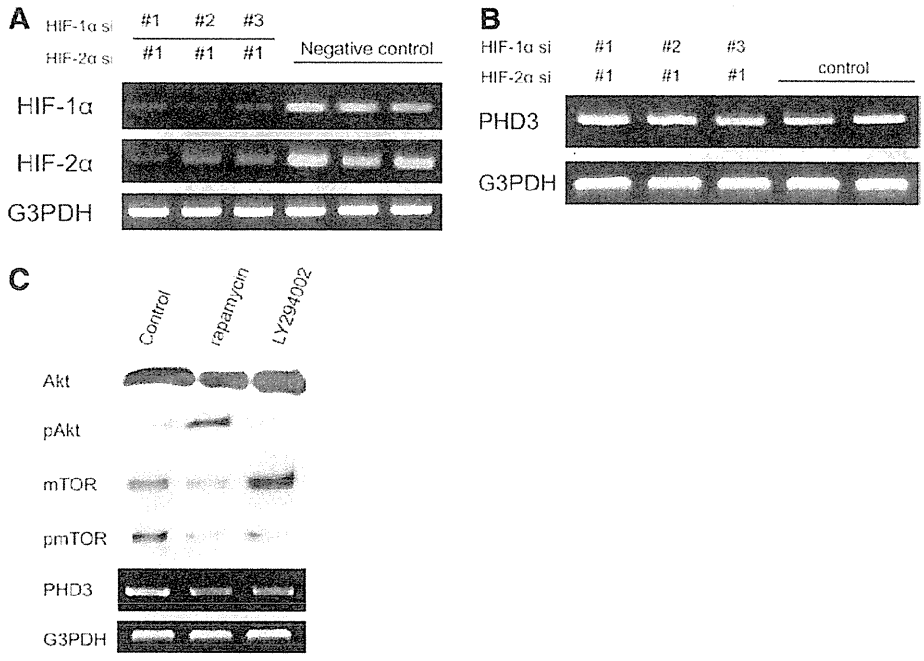

Fig. 2 HIF-protein-independent mechanism of PHD3 expression in Caki-1. **a** RT-PCR results of cotransfection of HIF-1α-targeted and HIF-2α-targeted siRNA into Caki-1. The HIF-1α-specific siRNAs, #1, #2 and #3 represent HSS104774, HSS104775 and HSS179231, respectively. The HIF-2α-specific siRNAs #1 represent HSS103261. **b** RT-PCR of PHD3 in HIF-1α/HIF-2α double-knockdown Caki-1 revealed no deterioration compared with the control. **c** Semiquantitative RT-PCR revealed that incubation with LY294002 and rapamycin attenuated PHD3 expression at the mRNA level in HIF-1α/HIF-2α double-knockdown Caki-1. Results of siRNAs using HSS104774 and HSS103261 are shown

PHD3 has an HIF-independent-antiproliferative function in renal cell carcinoma

The PI3K/Akt pathway might regulate PHD3 expression via proliferation signals. To verify the relationship between cell proliferation and PHD3 in RCC, we investigated the effect of PHD3si on cell proliferation by counting the cell number. Introducing PHD3-specific siRNA into Caki-1 significantly reduced the expression of PHD3 mRNA compared with control siRNA (Fig. 3a). The cell number was significantly increased, and the percentage of cells in the G0/G1 phase was decreased in Caki-1 treated with PHD3si compared

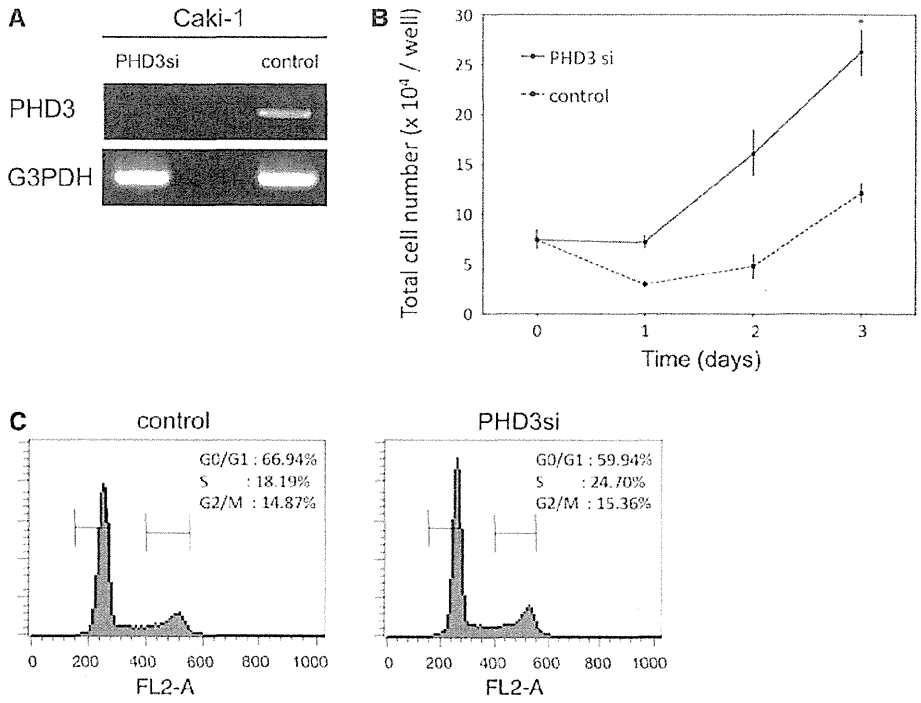

Fig. 3 In vitro acceleration of cell proliferation by PHD3 knockdown. **a** RT-PCR confirmed that PHD3 was silenced in Caki-1 transfected with a PHD3-specific siRNA (HSS132640). **b** Cell number was significantly increased in Caki-1 with PHD3-specific siRNA compared with the control. Data are shown as mean ± SEM of three independent experiments. $*p < 0.005$. **c** Flow cytometry shows a decrease in the percentage of cells in the G0/G1 phase in Caki-1 with PHD3-specific siRNA compared with the control

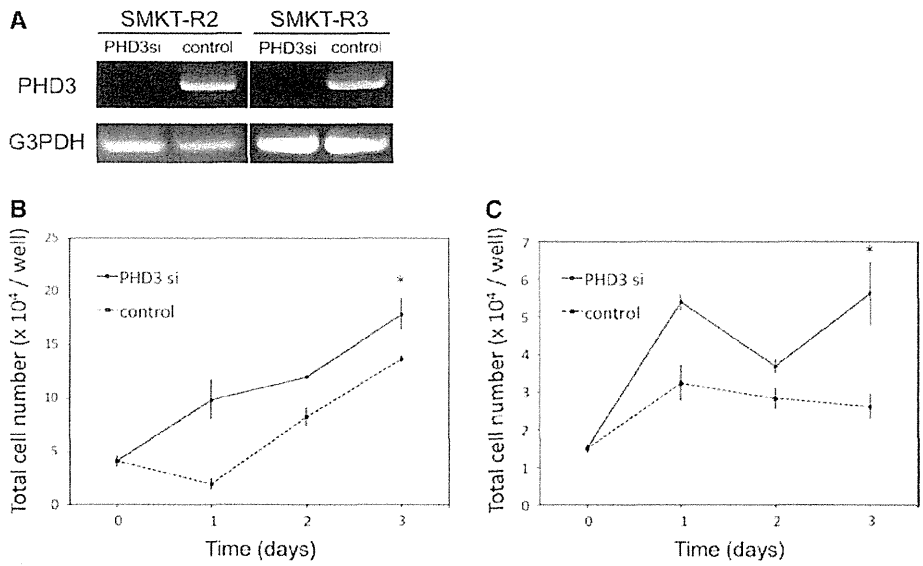

Fig. 4 In vitro cell proliferation promoted by PHD3 knockdown in VHL-mutant cell lines. **a** RT-PCR results of PHD3 in SMKT-R2 and SMKT-R3 with a PHD3-specific siRNA (HSS132640). **b** Cell number was significantly increased in SMKT-R2 with PHD3 targeting siRNA compared with the control. Data are shown as mean ± SEM of three independent experiments. $*p < 0.05$. **c** Cell number was significantly increased in SMKT-R2 with PHD3-targeting siRNA compared with control. Data are shown as mean ± SEM of three independent experiments. $*p < 0.05$

with the control (Fig. 3b, c). Subsequently, SMKT-R2 and SMKT-R3 VHL-mutant cells were transfected with PHD3-specific siRNA, and PHD3 expression was reduced compared with the control (Fig. 4a). Even in VHL-mutant cell lines SMKT-R2 and SMKT-R3, PHD3si significantly increased the number of cells (Fig. 4b, c). Cell proliferation was promoted both in VHL-intact and VHL-mutant cells by knockdown of PHD3, suggesting that intrinsic PHD3 had an antiproliferative effect. Then ACHN was transfected with the PHD3 expression vector (Fig. 5a). PHD3-expressing ACHN showed significantly lower cell proliferation than that with an empty vector (Fig. 5b). These results suggested that PHD3 had an antiproliferative effect that was independent of HIF protein and VHL gene status.

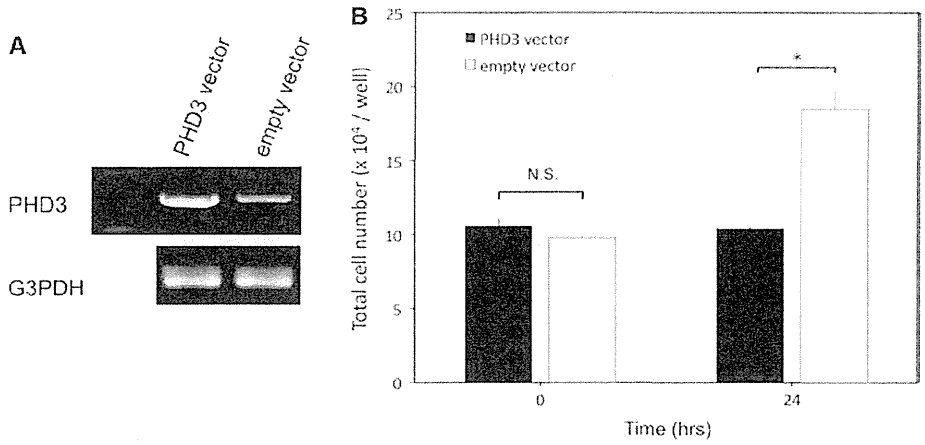

Fig. 5 In vitro deterioration of cell proliferation by gene transfection of PHD3. **a** RT-PCR revealed that PHD3 was overexpressed in ACHN transfected with the PHD3 plasmid compared with an empty vector. **b** Cell number was significantly decreased in ACHN with the PHD3 plasmid compared with the empty vector. Data are shown as mean ± SEM of three independent experiments. $^{*}p < 0.005$

PHD3 expression is an independent predictor of prolonged recurrence-free survival in CCRCC

Patients and tumor characteristics are shown in Table 1. PHD3-positive cells were observed in 82 (70.7 %) of the 116 cases (Fig. 6). The 5-year RFS rates were 90.8 and 69.9 % in patients with PHD3-positive and PHD3-negative tumors, respectively ($p = 0.0032$), although there was no significant difference in CSS between the 2 groups (Fig. 7). Multivariate analysis revealed that PHD3 expression was an independent predictor of favorable RFS when adjusted for known prognostic factors such as the pathological stage and Fuhrman grade (Table 2).

Table 1 Characteristics of the 116 patients

Characteristics	
Median age in years (range)	60 (28–85)
Median follow-up (months)	64
Sex	
Male	92 (79.3)
Female	24 (20.7)
ECOG PS	
0	102 (76.7)
1	27 (20.3)
2	3 (2.2)
3	1 (0.8)
Clinical stage	
Stage I	72 (54.1)
Stage II	9 (6.8)
Stage III	31 (23.3)
Stage IV	21 (15.8)
Fuhrman grade	
Grade 1	45 (33.8)
Grade 2	69 (51.9)
Grade 3	19 (14.3)
Grade 4	0 (0)

Values are *N* (%) except where indicated otherwise

Discussion

HIF was first identified as a regulator of hypoxia-induced erythropoietin expression (Semenza and Wang 1992; Wang et al. 1995; Wang and Semenza 1995). HIF-1α and HIF-2α are important regulators of tumor progression that induce more than 60 growth factors such as VEGF, platelet-derived growth factor, insulin-like growth factor, fibroblast growth factor and so on (Maynard and Ohh 2007). PHDs hydroxylate two conserved proline residues of HIF-1α and HIF-2α, leading to capture by the corresponding E3 ubiquitin–ligase VHL complex and degradation under normoxia, and lose the activity under hypoxia (Bruick and McKnight 2001; Cockman et al. 2000; Ivan et al. 2001; Jaakkola et al. 2001; Yu et al. 2001). As a result, PHDs control the activities of HIF protein under normoxic conditions. Therefore, it is considered that HIF-1α and HIF-2α can act only in a hypoxic microenvironment or cells with inactivated VHL protein.

The present study demonstrated two different mechanisms of PHD3 expression in RCCs that were observed under normoxia. RCC cell lines with VHL gene mutation had high expression of PHD3 under normoxia. This expression might be a feedback reaction from stable HIF protein accumulation. The mechanism possibly applies to CCRCC, which accounts for a large portion of RCCs (Aprelikova et al. 2004; Marxsen et al. 2004; Maxwell et al. 1999; Shinojima et al. 2007). Interestingly, normoxic expression of PHD3, which is regulated by a signal transduction pathway, could be seen in VHL-intact cells. Although the PI3 K/Akt pathway is a known regulator of HIF-1α expression (Blancher et al. 2001; Brugarolas et al. 2003; Hudson et al. 2002; Laughner et al. 2001; Pore et al. 2006; Zhong et al.

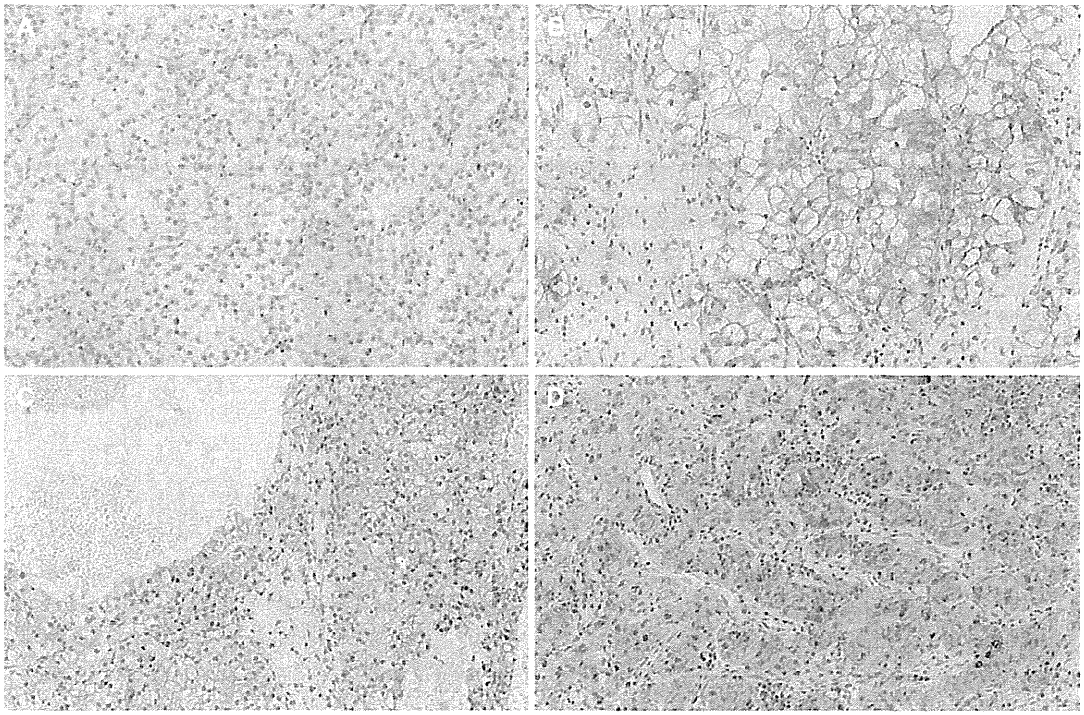

Fig. 6 Representative immunohistochemical staining of PHD3 in tumor tissue section of clear cell renal cell carcinoma. **a** Negative PHD3 expression in tumor cells. **b–d** Positive PHD3 expression in tumor cells

1998), we found that activation of the PI3K/Akt/mTOR pathway induced PHD3 expression irrespective of HIF protein accumulation. To the best of our knowledge, there has been no report proving an HIF-independent mechanism of PHD3 expression.

In this study, PHD3 silencing promoted proliferation of VHL-intact cells, although it did not induce HIF proteins accumulation, unlike PHD2 (Berra et al. 2003). Moreover, PHD3 silencing also promoted cell proliferation also in VHL-mutant cell lines, where HIF proteins were stably accumulated irrespective of hydroxylation. These results suggested that PHD3 had a direct antiproliferative function that was independent of HIF proteins and the VHL gene status in RCCs. In neuronal cells, PHD3 is induced after withdraw of nerve growth factor and promotes apoptosis (Lipscomb et al. 1999, 2001; Straub et al. 2003). However, this function is dependent on HIF-hydroxylase activity (Lee et al. 2005). Su et al. reported that PHD3 induced apoptosis independently of HIF-1 in pancreatic cancer (Su et al. 2010). In their report, the expression was induced and the apoptotic function enhanced under hypoxia. Our findings were in accord with their results in terms of the HIF-independent antiproliferative function. Moreover, our results suggested that PHD3 was expressed and suppressed cancer cell proliferation under normoxia in RCC, although this study has some limitations. The major one is that PHD3 expression was evaluated only by the mRNA level, not by the protein level in vitro, and the expression of mRNA does not always correlate with that of protein. In addition, we could not verify the expression mechanism and function of PHD3 in vivo because we could not obtain stable transfectants of cell lines with siRNA and the PHD3 gene. Although further investigation is needed to clarify the detailed mechanisms, results of the current study suggested that PHD3 was a potential antitumor molecule, which could be employed for gene or molecule target therapy irrespective of the VHL and HIF status and tissue oxygenic condition.

The results of the immunohistochemical study of PHD3 expression using primary tissue of CCRCC supported the view shown by the in vitro study, though the follow-up duration may have be insufficient to prove an impact on CSS, unlike RFS in this series. The expression of HIF-1α and -2α was not evaluated by immunohistochemistry in the present study. HIF protein expression should have been evaluated to indicate the concordance with the results of the in vitro study. However, the methods for evaluation of the expression are different among reports. Furthermore, positive rates of HIF-1α and HIF-2α also differ, ranging from 37–83 to 82–95 %, respectively (Atkins et al. 2005; Gordan et al. 2008; Klatte et al. 2007; Kroeze et al. 2010; Ku et al. 2011). Thus, it may be difficult to determine the association

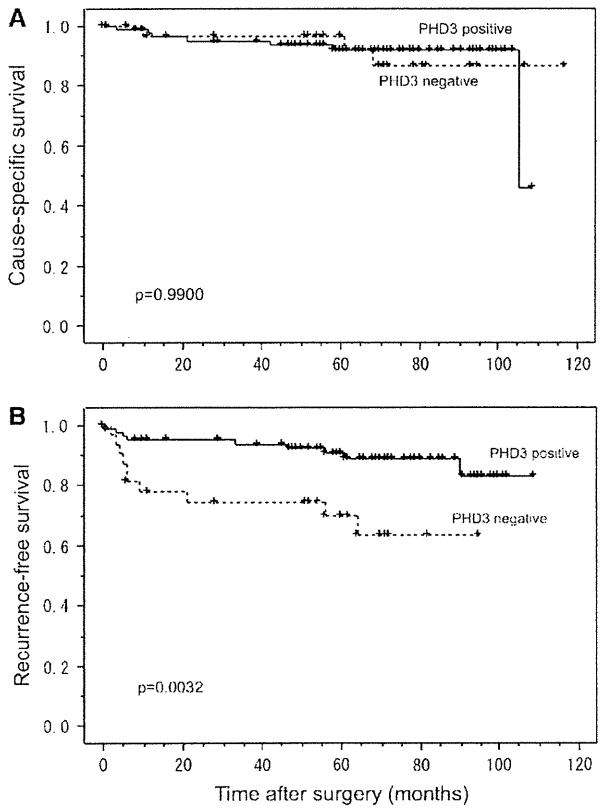

Fig. 7 Kaplan–Meier curves for cancer-specific survival (**a**) and recurrence-free survival (**b**) according to PHD3 status

Table 2 Prognostic factors for recurrence-free survival in univariate and multivariate analyses

	Univariate[a]		Multivariate[b]	
Factor	*n*	*p* value	*p* value	HR (95 % CI)
PHD3 positive	82	0.0032	0.0463	0.361 (0.133–0.983)
Fuhrman grade 3	12	0.0022	0.0365	3.331 (1.079–10.286)
Stage III or more	35	<0.0001	0.0042	4.837 (1.646–14.215)
Age >50 years	93	0.0852	0.4624	2.175 (0.274–17.274)
Female gender	24	0.9306	0.9795	1.015 (0.323–3.188)

HR hazard ratio, *CI* confidence interval

[a] Performed by using the log-rank test

[b] Done by using the Cox proportional hazard regression models

between the expression of PHD3 and that of HIF proteins by immunohistochemistry.

It is still unclear why PHD3, which can be induced through proliferative signals, has a paradoxical antiproliferative function. We speculate that PHD3 may play a role as a checkpoint mechanism in RCC cells that controls their growth and metabolites to adapt to the tissue environment. Commonly, CCRCC is known as a slow-growing tumor, and the majority of cases of CCRCC are discovered in the early stage and associated with a favorable prognosis (Volpe and Jewett 2005). High PHD3 expression may be consistent with this clinical feature. On the other hand, a few CCRCCs grow rapidly and are associated with poor prognosis. In some of these cases, a disturbance of PHD3 expression due to gene mutation or epigenetic processes may promote cell proliferation and correlate with tumor aggressiveness. To clarify this issue, further investigation is needed.

Conclusions

The results of the current study demonstrate that PHD3 expression can be induced in VHL-intact RCCs under normoxia via activation of the PI3 K/Akt/mTOR pathway independently of HIF-1α and HIF-2α. In addition, PHD3 has an antiproliferative function that is independent of HIF and VHL gene status. These findings reveal a novel expression mechanism and function of PHD3 in RCC.

Acknowledgments We thank Emiri Nakazawa, Akari Takahashi and Eri Saka for their skillful technical assistance, and Mr. Kim Barrymore for English correction of this manuscript. This study was supported in part by a grant-aid from Ministry of Education, Culture, Sports, Science and Technology of Japan.

Conflict of interest All authors of this paper reported no financial interests or potential conflict of interests.

References

Appelhoff RJ, Tian YM, Raval RR, Turley H, Harris AL, Pugh CW, Ratcliffe PJ, Gleadle JM (2004) Differential function of the prolyl hydroxylases PHD1, PHD2, and PHD3 in the regulation of hypoxia-inducible factor. J Biol Chem 279:38458–38465

Aprelikova O, Chandramouli GV, Wood M, Vasselli JR, Riss J, Maranchie JK, Linehan WM, Barrett JC (2004) Regulation of HIF prolyl hydroxylases by hypoxia-inducible factors. J Cell Biochem 92:491–501

Atkins DJ, Gingert C, Justenhoven C, Schmahl GE, Bonato MS, Brauch H, Störkel S (2005) Concomitant deregulation of HIF1a and cell cycle proteins in VHL-mutated renal cell carcinomas. Virchows Arch 447:634–642

Berra E, Benizri E, Ginouves A, Volmat V, Roux D, Pouyssegur J (2003) HIF prolyl-hydroxylase 2 is the key oxygen sensor setting low steady-state levels of HIF-1a in normoxia. EMBO J 22:4082–4090

Blancher C, Moore JW, Robertson N, Harris AL (2001) Effects of ras and von Hippel-Lindau (VHL) gene mutations on hypoxia-inducible factor (HIF)-1α, HIF-2α, and vascular endothelial growth factor expression and their regulation by the phosphatidylinositol 3′-kinase/Akt signaling pathway. Cancer Res 61:7349–7355

Brugarolas JB, Vazquez F, Reddy A, Sellers WR, Kaelin WG Jr (2003) TSC2 regulates VEGF through mTOR-dependent and -independent pathways. Cancer Cell 4:147–158

Bruick RK, McKnight SL (2001) A conserved family of prolyl-4-hydroxylases that modify HIF. Science 294:1337–1340

Cioffi CL, Liu XQ, Kosinski PA, Garay M, Bowen BR (2003) Differential regulation of HIF-1α prolyl-4-hydroxylase genes by hypoxia in human cardiovascular cells. Biochem Biophys Res Commun 303:947–953

Cockman ME, Masson N, Mole DR, Jaakkola P, Chang GW, Clifford SC, Maher ER, Pugh CW, Ratcliffe PJ, Maxwell PH (2000) Hypoxia inducible factor-a binding and ubiquitylation by the von Hippel-Lindau tumor suppressor protein. J Biol Chem 275:25733–25741

del Peso L, Castellanos MC, Temes E, Martin-Puig S, Cuevas Y, Olmos G, Landazuri MO (2003) The von Hippel Lindau/hypoxia-inducible factor (HIF) pathway regulates the transcription of the HIF-proline hydroxylase genes in response to low oxygen. J Biol Chem 278:48690–48695

Edge SB, Byrd DR, Compton CC, Fritz AG, Greene FL, Trotti A (2010) American Joint Committee on Cancer (AJCC) staging manual, 7th edn. Springer, Philadelphia

Fuhrman S, Lasky LC, Limas L (1982) Prognostic significance of morphologic parameters in renal cell carcinoma. Am J Surg Pathol 6:655

Gordan JD, Lal P, Dondeti VR, Letrero R, Parekh KN, Oquendo CE, Greenberg RA, Flaherty KT, Rathmell WK, Keith B, Simon MC, Nathanson KL (2008) HIF-α effects on c-Myc distinguish two subtypes of sporadic VHL-deficient clear cell renal carcinoma. Cancer Cell 14:435–446

Hirsila M, Koivunen P, Gunzler V, Kivirikko KI, Myllyharju J (2003) Characterization of the human prolyl 4-hydroxylases that modify the hypoxia-inducible factor. J Biol Chem 278:30772–30780

Huang J, Zhao Q, Mooney SM, Lee FS (2002) Sequence determinants in hypoxia-inducible factor-1a for hydroxylation by the prolyl hydroxylases PHD1, PHD2, and PHD3. J Biol Chem 277:39792–39800

Hudson CC, Liu M, Chiang GG, Otterness DM, Loomis DC, Kaper F, Giaccia AJ, Abraham RT (2002) Regulation of hypoxia-inducible factor 1a expression and function by the mammalian target of rapamycin. Mol Cell Biol 22:7004–7014

Ivan M, Kondo K, Yang H, Kim W, Valiando J, Ohh M, Salic A, Asara JM, Lane WS, Kaelin WG Jr (2001) HIFα targeted for VHL-mediated destruction by proline hydroxylation: implications for O2 sensing. Science 292:464–468

Jaakkola P, Mole DR, Tian YM, Wilson MI, Gielbert J, Gaskell SJ, von Kriegsheim A, Hebestreit HF, Mukherji M, Schofield CJ, Maxwell PH, Pugh CW, Ratcliffe PJ (2001) Targeting of HIF-α to the von Hippel-Lindau ubiquitylation complex by O2-regulated prolyl hydroxylation. Science 292:468–472

Klatte T, Seligson DB, Riggs SB, Leppert JT, Berkman MK, Kleid MD, Yu H, Kabbinavar FF, Pantuck AJ, Belldegrun AS (2007) Hypoxia-inducible factor 1α in clear cell renal cell carcinoma. Clin Cancer Res 13:7388–7393

Kroeze SG, Vermaat JS, van Brussel A, van Melick HH, Voest EE, Jonges TG, van Diest PJ, Hinrichs J, Bosch JL, Jans JJ (2010) Expression of nuclear FIH independently predicts overall survival of clear cell renal cell carcinoma patients. Eur J Cancer 46:3375–3382

Ku JH, Park YH, Myung JK, Moon KC, Kwak C, Kim HH (2011) Expression of hypoxia inducible factor-1α and 2α in conventional renal cell carcinoma with or without sarcomatoid differentiation. Urol Oncol 29:731–737

Laughner E, Taghavi P, Chiles K, Mahon PC, Semenza GL (2001) HER2 (neu) signaling increases the rate of hypoxia-inducible factor 1α (HIF-1α) synthesis: novel mechanism for HIF-1-mediated vascular endothelial growth factor expression. Mol Cell Biol 21:3995–4004

Lee S, Nakamura E, Yang H, Wei W, Linggi MS, Sajan MP, Farese RV, Freeman RS, Carter BD, Kaelin WG Jr, Schlisio S (2005) Neuronal apoptosis linked to EglN3 prolyl hydroxylase and familial pheochromocytoma genes: developmental culling and cancer. Cancer Cell 8:155–167

Lieb ME, Menzies K, Moschella MC, Ni R, Taubman MB (2002) Mammalian EGLN genes have distinct patterns of mRNA expression and regulation. Biochem Cell Biol 80:421–426

Lipscomb E, Sarmiere P, Crowder R, Freeman RS (1999) Expression of the SM-20 gene promotes death in nerve growth factor-dependent sympathetic neurons. J Neurochem 73:429–432

Lipscomb E, Sarmiere P, Freeman RS (2001) SM-20 is a novel mitochondrial protein that causes caspase-dependent cell death in nerve growth factor-dependent neurons. J Biol Chem 276:11775–11782

Marxsen JH, Stengel P, Doege K, Heikkinen P, Jokilehto T, Wagner T, Jelkmann W, Jaakkola P, Metzen E (2004) Hypoxia-inducible factor-1 (HIF-1) promotes its degradation by induction of HIF-α-prolyl-4-hydroxylases. Biochem J 381:761–767

Maxwell PH, Wiesener MS, Chang GW, Clifford SC, Vaux EC, Cockman ME, Wykoff CC, Pugh CW, Maher ER, Ratcliffe PJ (1999) The tumour suppressor protein VHL targets hypoxia-inducible factors for oxygen-dependent proteolysis. Nature 399:271–275

Maynard MA, Ohh M (2007) The role of hypoxia-inducible factors in cancer. Cell Mol Life Sci 64:2170–2180

Pescador N, Cuevas Y, Naranjo S, Alcaide M, Villar D (2005) Landázuri MO, del Peso L: identification of a functional hypoxia-responsive element that regulates the expression of the egl nine homologue 3 (egln3/phd3) gene. Biochem J 390:189–197

Pore N, Jiang Z, Shu HK, Bernhard E, Kao GD, Maity A (2006) Akt1 activation can augment hypoxia-inducible factor-1a expression by increasing protein translation through a mammalian target of rapamycin-independent pathway. Mol Cancer Res 4:471–479

Sato E, Torigoe T, Hirohashi Y, Kitamura H, Tanaka T, Honma I, Asanuma H, Harada K, Takasu H, Masumori N, Ito N, Hasegawa T, Tsukamoto T, Sato N (2008) Identification of an immunogenic CTL epitope of HIFPH3 for immunotherapy of renal cell carcinoma. Clin Cancer Res 14:6916–6923

Semenza GL, Wang GL (1992) A nuclear factor induced by hypoxia via de novo protein synthesis binds to the human erythropoietin gene enhancer at a site required for transcriptional activation. Mol Cell Biol 12:5447–5454

Shinojima T, Oya M, Takayanagi A, Mizuno R, Shimizu N, Murai M (2007) Renal cancer cells lacking hypoxia-inducible factor (HIF)-1α expression maintain vascular endothelial growth factor expression through HIF-2α. Carcinogenesis 28:529–536

Straub JA, Lipscomb EA, Yoshida ES, Freeman RS (2003) Induction of SM-20 in PC12 cells leads to increased cytochrome c levels, accumulation of cytochrome c in the cytosol, and caspase-dependent cell death. J Neurochem 85:318–328

Su Y, Loos M, Giese N, Hines OJ, Diebold I, Görlach A, Metzen E, Pastorekova S, Friess H, Büchler P (2010) PHD3 regulates differentiation, tumour growth and angiogenesis in pancreatic cancer. Br J Cancer 103:1571–1579

Tanaka T, Kitamura H, Torigoe T, Hirohashi Y, Sato E, Masumori N, Sato N, Tsukamoto T (2011) Autoantibody against hypoxia-inducible factor prolyl hydroxylase-3 is a potential serological marker for renal cell carcinoma. J Cancer Res Clin Oncol 137:789–794

Volpe A, Jewett MAS (2005) The natural history of small renal masses. Nat Clin Pract Urol 2:384–390

Wang GL, Semenza GL (1995) Purification and characterization of hypoxia-inducible factor 1. J Biol Chem 270:1230–1237

Wang GL, Jiang BH, Rue EA, Semenza GL (1995) Hypoxia-inducible factor 1 is a basic-helix-loop-helix-PAS heterodimer regulated by cellular O2 tension. Proc Natl Acad Sci USA 92:5510–5514

Yamamoto M, Torigoe T, Kamiguchi K, Hirohashi Y, Nakanishi K, Nabeta C, Asanuma H, Tsuruma T, Sato T, Hata F, Ohmura T, Yamaguchi K, Kurotaki T, Hirata K, Sato N (2005) A novel

isoform of TUCAN is overexpressed in human cancer tissues and suppresses both caspase-8- and caspase-9-mediated apoptosis. Cancer Res 65:8709–8714

Yu F, White SB, Zhao Q, Lee FS (2001) HIF-1α binding to VHL is regulated by stimulus-sensitive proline hydroxylation. Proc Natl Acad Sci USA 98:9630–9635

Zhong H, Agani F, Baccala AA, Laughner E, Rioseco-Camacho N, Isaacs WB, Simons JW, Semenza GL (1998) Increased expression of hypoxia inducible factor-1a in rat and human prostate cancer. Cancer Res 58:5280–5284

Cancer Science
Japanese Cancer Association JCA
Open Access

Heat shock protein DNAJB8 is a novel target for immunotherapy of colon cancer-initiating cells

Rena Morita,[1] Satoshi Nishizawa,[1,2] Toshihiko Torigoe,[1] Akari Takahashi,[1] Yasuaki Tamura,[1] Tomohide Tsukahara,[1] Takayuki Kanaseki,[1] Alice Sokolovskaya,[1] Vitaly Kochin,[1] Toru Kondo,[3] Satoshi Hashino,[4] Masahiro Asaka,[5] Isao Hara,[2] Yoshihiko Hirohashi[1] and Noriyuki Sato[1]

[1]Department of Pathology, Sapporo Medical University School of Medicine, Sapporo; [2]Department of Urology, Wakayama Medical University School of Medicine, Wakayama; [3]Department of Stem Cell Biology; [4]Health Administration Center; [5]Department of Cancer Preventive Medicine, Hokkaido University Graduate School of Medicine, Sapporo, Japan

Key words

Cancer immunotherapy, cancer stem-like cell, colorectal cancer, DNAJB8, tumor antigen

Correspondence

Yoshihiko Hirohashi or Toshihiko Torigoe, Department of Pathology, Sapporo Medical University School of Medicine, South-1 West-17, Chuo-Ku, Sapporo 060-8556, Japan.
Tel: +81-1-1611-2111 (ext. 2692); Fax: +81-1-1643-2310;
E-mails: hirohash@sapmed.ac.jp; torigoe@sapmed.ac.jp

Funding information

Ministry of Education, Culture, Sports, Science and Technology of Japan. Takeda Science Foundation. Japan Society for the Promotion of Science for Young Scientists.

Received December 15, 2013; Revised January 16, 2014; Accepted January 20, 2014

Cancer Sci **105** (2014) 389–395

doi: 10.1111/cas.12362

The aim of the present study was to establish cancer stem-like cell/cancer-initiating cell (CSC/CIC)-targeting immunotherapy. The CSC/CIC are thought to be essential for tumor maintenance, recurrence and distant metastasis. Therefore they are reasonable targets for cancer therapy. In the present study, we found that a heat shock protein (HSP) 40 family member, DnaJ (Hsp40) homolog, subfamily B, member 8 (DNAJB8), is preferentially expressed in CSC/CIC derived from colorectal cancer (CRC) cells rather than in non-CSC/CIC. Overexpression of DNAJB8 enhanced the expression of stem cell markers and tumorigenicity, indicating that DNAJB8 has a role in CRC CSC/CIC. A DNAJB8-specific cytotoxic T lymphocyte (CTL) response could be induced by a DNAJB8-derived antigenic peptide. A CTL clone specific for DNAJB8 peptide showed higher killing activity to CRC CSC/CIC compared with non-CSC/CIC, and CTL adoptive transfer into CRC CSC/CIC showed an antitumor effect *in vivo*. Taken together, the results indicate that DNAJB8 is expressed and has role in CRC CSC/CIC and that DNAJB8 is a novel target of CRC CSC/CIC-targeting immunotherapy.

Colorectal cancer (CRC) is one of the major malignant diseases worldwide and has the second-highest mortality rate in the United States.[1] Although recent approaches have achieved improvements in CRC treatment including novel combination chemotherapies and molecular-targeting therapies, the prognosis of patients with metastasis and recurrence is still poor. Thus, development of therapy for advanced CRC is an urgent task. Cancer stem-like cells/cancer-initiating cells (CSC/CIC) are defined by their ability of tumor initiation, self-renewal and differentiation.[2] It has been reported that CSC/CIC are resistant to chemotherapy and radiotherapy.[3] The CSC/CIC with these features are considered to be related to metastasis and recurrence and to be important therapeutic targets.

Immunotherapy for cancer has attracted much attention as a new strategy compared with traditional therapies such as chemotherapy and radiotherapy. Identification of the first human tumor-associated antigens (TAA) in the early 1990s enabled cancer immunotherapies using antigenic peptides derived from TAA.[4] Some peptide vaccination trials showed fascinating results; however, there are also pessimistic opinions.[5,6] Our previous trials using a Survivn 2B-derived peptide vaccine showed partial clinical benefits for some cancer patients, but the results were not sufficiently satisfactory.[7–12] There are many reasons why peptide vaccine therapies are not so effective in clinical settings, one of the main reasons being antigen loss on cancer cells. Therefore, the ideal targets for cancer immunotherapy are thought to be TAA that have critical functions for CSC/CIC maintenance, since CSC/CIC have a high tumor-initiating ability.[13]

DnaJ (Hsp40) homolog, subfamily B, member 8 (DNAJB8) belongs to the heat shock protein (HSP) 40 family. The HSP40 family proteins are co-chaperones of HSP70 and DNAJB8 has a role in suppression of misfolded toxic protein aggregation.[14] Recently, it has been reported that some members of the HSP40 family are related to the development and metastasis of cancers and that their expression was detected in breast cancer stem cells.[15] We found that DNAJB8 was expressed preferentially in CSC/CIC derived from renal cell carcinoma. DNAJB8 was expressed only in the testis among normal tissues and thus it is a novel cancer/testis antigen. Moreover, we confirmed its immunogenicity by using a mice DNA vaccination model, indicating that DNAJB8 is a promising target of CSC/CIC-targeting immunotherapy.[16] However, it is not clear whether DNAJB8 is expressed in human CSC/CIC of other cancers, including CRC. In the present study, we analyzed the expression and functions of DNAJB8 in CRC and the potency of DNAJB8 as a target for CRC CSC/CIC-targeting immunotherapy.

Materials and Methods

Cell lines. Colon adenocarcinoma cell lines SW480 (HLA-A*0201/2402), HT29 (HLA-A*0101/2403) and HCT15 (HLA-A*0201/2402) were kind gifts from Dr K. Imai (Sapporo, Japan). All cells were cultured in DMEM (Sigma-Aldrich, St Louis, MO, USA) supplemented with 10% fetal bovine serum (FBS) (Life Technologies, Carlsbad, CA, USA). The erythroleukemia cell line K562 was purchased from ATCC (Manassas, VA, USA) and was cultured in RPMI-1640 (Sigma-Aldrich) supplemented with 10% FBS. The HLA-A*2402 stably transfected transporter associated with antigen processing (TAP)-deficient cell line T2A-A*2402 (T2-A24) was a kind gift from Dr K. Kuzushima (Nagoya, Japan) and was cultured in RPMI-1640 supplemented with 10% FBS and 0.8 mg/mL G418 (Life Technologies).

Retroviral gene transduction and generation of stable transformants. Transduction of genes into cells was carried out using a retrovirus-mediated method as described previously.[16] PLAT-A cells (a kind gift from Dr T. Kitamura, Tokyo, Japan), which are amphotropic packaging cells, were transiently transduced with a pMXs-puro retroviral vector expressing *DNAJB8* and a control plasmid using Lipofectamine 2000 reagent (Life Technologies) following the manufacturer's protocol. Retroviral supernatants were harvested 48 h after transfection. The supernatant was used for infection of HT29 cells in the presence of 8 mg/mL of polybrene (Sigma-Aldrich) overnight. For the generation of stable transformants, the infected cells were selected with 1 μg/mL puromycin. DNAJB8 expression was confirmed using western blot analysis.

Side population (SP) analysis. The SP analysis was performed as described previously.[16–18] The cells were labeled with Hoechst 33342 dye (Lonza, Walkersville, MD, USA) for 90 min at concentrations of 10 μg/mL for HCT15, 7.5 μg/mL for HT29 and 5 μg/mL for SW480 with or without Verapamil (Sigma-Aldrich), which is an inhibitor of ATP-binding cassette (ABC) transporters, at concentrations of 100 μM for HT29 and 50 μM for SW480 and HCT15. Cells were counterstained with 1 μg/mL propidium iodide (Sigma-Aldrich) for labeling dead cells. Viable cells were sorted using a BD FACS Aria II Cell-Sorting System (BD, Franklin Lakes, NJ, USA).

Xenograft model. All mouse procedures were carried out in accordance with institutional protocol guidelines at Sapporo Medical University School of Medicine. The SP cells and presorted cells from colon cancer cell lines were mixed with Matrigel (BD) at a 1:1 volume and injected subcutaneously into the back of 4–8-week-old female non-obese diabetic /severe combined immunodeficiency (NOD/SCID) mice. Tumor size was assessed weekly using a caliper and calculated using the following formula: tumor size (mm^3) = (longest diameter × shortest $diameter^2$)/2.

RT-PCR analysis and quantitative RT-PCR analysis. RT-PCR analysis was performed as described previously.[16] Total RNA (tRNA) were isolated from SP, main population (MP) and unsorted cells using an RNeasy Mini Kit (Qiagen, Valencia, CA, USA) according to the manufacturer's protocol. Complementary DNA (cDNA) was synthesized from 2 μg of total RNA by reverse transcription using Superscript III reverse transferase (Invitrogen, Palo Alto, CA, USA). A cDNA panel for a set of normal human adult tissues and fetal tissues was purchased from Clontech (Mountain View, CA, USA). RT-PCR was performed in 20 μL of PCR mixture containing 1 μL of cDNA mixture, 0.5 μL of Taq DNA polymerase (Qiagen, Valencia, CA, USA) and 4 pmol of primers. The PCR mixture was initially incubated at 94°C for 2 min, followed by 35 cycles of denaturation at 94°C for 15 s, annealing at 58°C for 30 s and extension at 72°C for 30 s. The primer pairs used for RT-PCR analysis were 5′-CATGATGGAGACGGAGCTGA-3′ and 5′-ACCCCGCTCGCCATGCTATT-3′ for *SOX2* with an expected PCR product size of 410 base pairs (bp), 5′-AG CTCTGTGGACTGCTGGTT-3′ and 5′-GGACGCCAGTTG CAAAGTAT-3′ for *DNAJB8* with an expected PCR product size of 409 bp, 5′-CCCGACAAGAACCCTGACAAT-3′ and 5′-AGGTGGATGAGAAGGTGGTG-3′ for *POU5F1* with an expected PCR product size of 163 bp, 5′-CTCTTCCTCAA ACCGTCTGC-3′ and 5′-GATCGGAGGCTAAGCAACTG-3′ for *LGR5* with an expected PCR product size of 181 bp and 5′-ACCACAGTCCATGCCATCAC-3′ and 5′-TCCACCACCC TGTTGCTGTA-3′ for *glyceraldehyde-3-phosphate dehydrogenase* (*GAPDH*) with an expected product size of 452 bp. Quantitative real-time PCR was performed using an ABI PRISM 7000 sequence detection system (Life Technologies) according to the manufacturer's protocol. Primers and probes were designed by the manufacturer (TaqMan gene expression assays; Life Technologies). Thermal cycling was performed using 40 cycles of denaturation at 95°C for 15 s followed by annealing at 60°C for 1 min. Each experiment was performed in triplicate, with normalization to the *GAPDH* gene as an internal control.

Sphere formation assay. To assay sphere formation efficiency, 10^3 cells were plated in Ultra Low Attachment six-well plates (Corning Incorporated Life Sciences, Acton, MA, USA) and cultured in Dulbecco's modified Eagle's medium/F12 (Life Technologies) supplemented with 20 ng/mL epidermal growth factor and 20 ng/mL basic fibroblast growth factor (R&D Systems, Minneapolis, MN, USA). The cells were incubated in a 5% CO_2 incubator for 2 weeks and the number of spheres was counted under a microscope in 15 low-power fields and then the average was calculated.

Synthetic peptides and peptide binding assay. Putative antigenic peptides can be designed using several website programs, such as BIMAS (http://www-bimas.cit.nih.gov/molbio/hla_bind/). Four peptides, DNAJB8_22(8) (AYRKLALRW), DNAJB8_90 (10) (GYTFRNPEDI), DNAJB8_99(9) (IFREFFGGL) and DNAJB8_143(9) (AFMEAFSSF), were designed from the amino acid sequence of DNAJB8 according to the HLA-A24-binding motifs.

Peptide binding affinity to HLA-A24 was assessed using HLA-A24 a stabilization assay as described previously.[19] Survivin-2B_80(9) (AYACNTSTL) peptide was used as a positive control and SL8C (SIINFEKL), which is a H2-K^b-binding peptide derived from Ovalbumin protein, was used as a negative control.

Cytotoxic T lymphocyte (CTL) induction and establishment of CTL clone. The PBMC were isolated from two healthy volunteer donors, from whom we obtained informed consent according to the guidelines of the Declaration of Helsinki, using standard density gradient centrifugation on Lymphoprep (Nycomed, Oslo, Norway). Isolation of $CD8^+$ cells and establishment of phytohaemagglutinin (PHA) blast were performed as described previously.[20,21]

The CTL induction was performed as described previously.[20,21] $CD8^+$ T cells were stimulated with a peptide-pulsed PHA blast for 2–3 times weekly. On day 21, $CD8^+$ T cell reactivity was assessed using interferon (IFN)-γ enzyme-linked immunospot (ELISpot) assay. On day 28, the cytotoxic activity of T cells was assessed using a conventional 6-h ^{51}Cr

release assay. To obtain CTL clones, standard limiting dilution was performed as described previously.[21]

Interferon-γ ELISpot assay and cytotoxicity assay. An IFN-γ ELISpot assay was performed as described previously.[21] $CD8^+$ T cells, 2×10^5, were incubated with 5×10^4/well T2-A24 cells pulsed with each peptide (50 μg/mL) or K562 cells. After incubation for 40 h at 37°C, IFN-γ spots were developed and counted as per the manufacturer's instructions.

The lytic activity of CTL was tested using a ^{51}Cr release assay as described previously.[20,21] ^{51}Cr-labeled target cells (2000 cells/well) were incubated with various numbers of effector cells for 6 h at 37°C in 96-well microtiter plates and the cytotoxicity was calculated with radioactivity of the culture supernatants.

Cytotoxic T lymphocyte adoptive transfer. Fifteen NOD/SCID mice were inoculated subcutaneously in the back with 1×10^5 HT29 cells. Three weeks later, when the tumors were palpable, 1×10^4 or 1×10^3 DNAJB8_143(9)-specific CTL clone cells or PBS was injected intravenously into five mice for each group. The same adoptive transfer procedure was performed 2 weeks after inoculation with SP cells. Tumor size was assessed weekly.

Statistical analysis. In the xenograft model, cytotoxicity assay and CTL adoptive transfer model, samples were analyzed using Student's *t*-test, with $P < 0.05$ conferring statistical significance.

Results

Expression of DNAJB8 in CRC CSC/CIC. Human CRC CSC/CIC have previously been isolated from CRC cell lines and primary CRC samples using several methods, including the use of cell surface markers (e.g. CD133), SP cells using Hoechst 33342 analysis and the Aldefluor assay.[22–26] In the present study, we isolated CRC CSC/CIC using SP cell analysis. Although previous studies showed that some colon cancer SP cells were not enriched with a CSC/CIC population,[27] our previous study confirmed that SW480, HT29 and HCT15 SP cells had high tumor-initiating ability, high expression levels of stem cell markers such as *SOX2* and *POU5F1* and strong resistance to chemotherapeutic agents compared with MP cells.[18] The ratio of SW480 SP cells was 4.0%, that of HCT15 cells was 5.5% and that of HT29 cells was 0.8%. All of these SP cells were specifically inhibited by verapamil, an ABC transporter inhibitor (Fig. 1a). Expression of *DNAJB8* mRNA in SP cells and MP cells was examined using RT-PCR. *DNAJB8* mRNA was detected in SP cells derived from SW480, HCT15 and HT29 cells, whereas *DNAJB8* mRNA was not detected in MP cells (Fig. 1b). Thus, DNAJB8 is one candidate of CSC/CIC-specific antigens in CRC as well as in renal cell carcinomas. *DNAJB8* mRNA was detected in SP cells derived from HT29 cells at the highest level (Fig. 1b) and therefore HT29 cells were used for further analysis. The quality of SP cells derived from HT29 cells as a source of CRC CSC/CIC was confirmed by higher expression levels of stem cell markers, including *SOX2*, *POU5F1* and *LGR5*, using RT-PCR and by a higher tumor-initiating ability in a xenograft model than those of MP cells (Fig. 1c, d).

Role of DNAJB8 in CRC CSC/CIC. To evaluate the functions of DNAJB8 in HT29 cells, we established DNAJB8-overexpressed cells. We confirmed the overexpression of *DNAJB8* mRNA using quantitative RT-PCR (Fig. 2a). Expression levels of the stem cell markers SOX2, LGR5 and POU5F1 were increased by 2.2-fold, 2.3-fold and 2.1-fold, respectively, in *DNAJB8*-overexpressed HT29 cells compared with the level in the control HT29 cells (Fig. 2a). The percentage of SP cells in *DNAJB8*-overexpressed HT29 cells was higher than that in control HT29 cells (Fig. 2b). To confirm the tumorigenicity *in vivo* of *DNAJB8*-overexpressed HT29 cells, we used a xenograft transplantation model. The *DNAJB8*-overexpressed HT29 cells showed higher tumor-initiating ability compared with HT29 control cells (Fig. 2c). A sphere formation assay was used to evaluate CSC/CIC-like features. *DNAJB8*-overexpressed HT29 cells showed higher sphere-forming ability than that of HT29 control cells (Fig. 2d), indicating that overexpression of DNAJB8 induced CSC/CIC properties.

Establishment of DNAJB8-targeting immunotherapy. To verify the immunogenicity for peptides from DNAJB8 protein, DNAJB8-specific CTL were induced using HLA-A*2402-positive healthy volunteer donors. Candidate antigenic peptides carrying the HLA-A*2402-binding anchor motif were screened according to the amino acid sequence of DNAJB8 protein and there were four candidate peptides (DNAJB8_22[8], DNAJB8_90[10], DNAJB8_99[9] and DNAJB8_143[9]) (Fig. 3). The HLA-A24 binding ability was then assessed using a HLA-A24 binding assay with SL8C peptide as a negative control and Survivin-2B_80(9) as a positive control. DNAJB8_22(9), DNAJB8_99(9) and DNAJB8_143(9) showed ability to bind to HLA-A24, whereas DNAJB8_90(10) did not (Fig. 3). Therefore, DNAJB8_22(9), DNAJB8_99(9) and DNAJB8_143(9) peptides were used for further CTL induction experiments.

The PBMC of two healthy volunteer donors (A and B) were stimulated using a mixture of DNAJB8_22(9), DNAJB8_99(9) and DNAJB8_143(9) and then the reactivity for each peptide was evaluated using a IFN-γ ELISpot assay and ^{51}Cr release assay. Interferon-γ secretion was observed for DNAJB8_22(8)-pulsed and DNAJB8_143(9)-pulsed target cells from both donors using a IFN-γ ELISpot assay (Fig. 4a), whereas cytotoxic activity was detectable for only DNAJB8_143(9)-pulsed target cells using a ^{51}Cr release assay (Fig. 4b). Therefore, DNAJB8_143(9) peptide is a candidate for DNAJB8-targeting immunotherapy. We generated four CTL clones specific for DNAJB8_143(9) from donor A (CTL clone #21, 67 and 84) and one clone from donor B (CTL clone #70) and performed further analysis using CTL clone #84. The DNAJB8_143(9)-specific CTL clone showed cytotoxic activity for T2-A24 cells pulsed with DNAJB8_143(9) peptide but not for T2-A24 cells without the peptide or for K562 cells (Fig. 4c). To verify whether this CTL clone can recognize endogenously presented DNAJB8_143(9) peptide of DNAJB8-positive CRC CSC/CIC, we performed a ^{51}Cr release assay using SP cells derived from HT29 cells. The DNAJB8_143(9)-specific CTL clone showed greater cytotoxic activity for HLA-A*2402+ HT29-SP cells than for HLA-A*2402+ HT29-MP cells or HLA-A*2402-DNAJB8- K562 cells (Fig. 4d). These results indicate that DNAJB8_143(9) peptide is an immunogenic epitope and that the endogenously processed peptide is presented on the surface of SP cells.

Finally, we evaluated the antitumor effect *in vivo* of the DNAJB8-specific CTL clone using a therapeutic CTL adoptive transfer model. The DNAJB8-CTL clone-transferred group showed a significant antitumor effect compared with that in the control group (Fig. 4e). The group with 10^4 CTL injection showed a tendency for a greater antitumor effect than that in the group with 10^3 CTL injection. These results indicate that DNAJB8_143(9) peptide is an immunogenic epitope and is a candidate for CRC CSC/CIC-targeting immunotherapy.

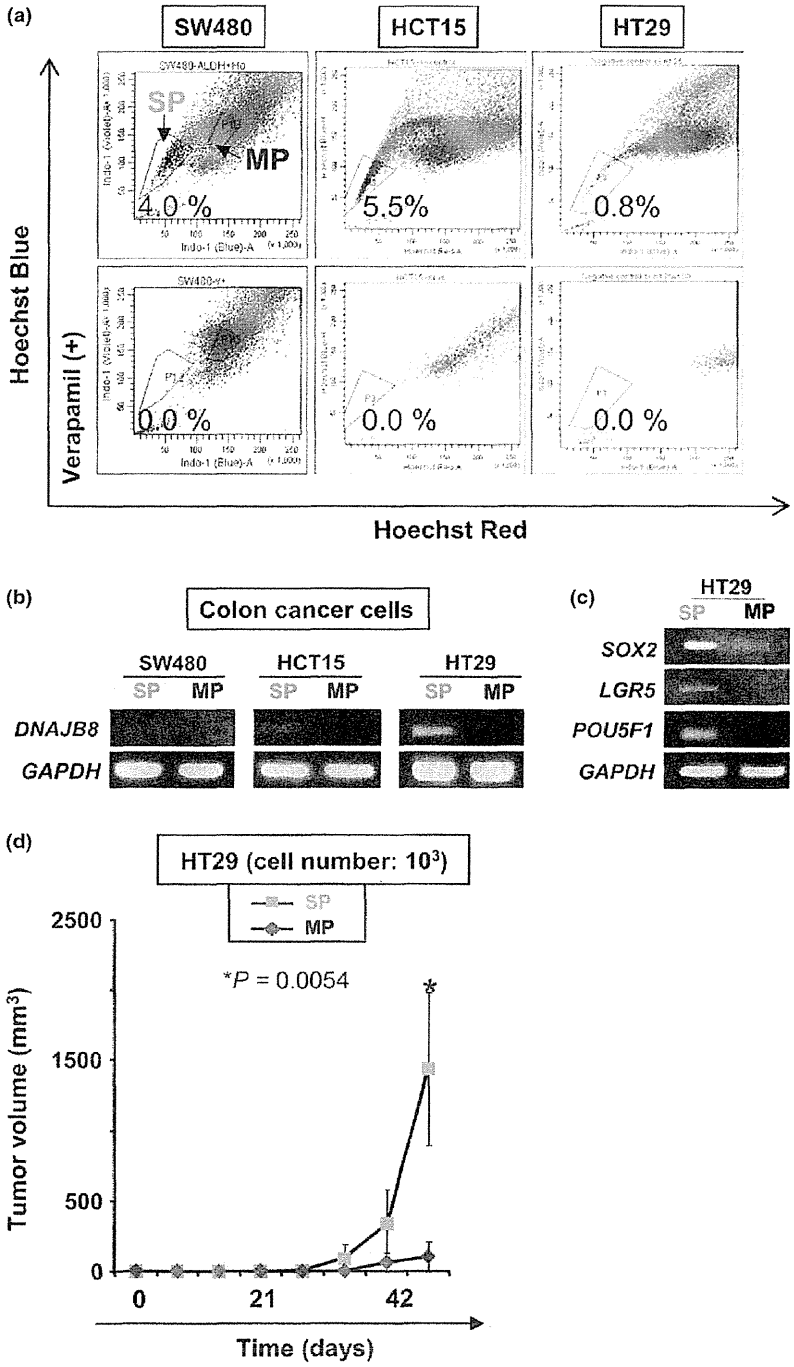

Fig. 1. Isolation of colon cancer stem-like cells/cancer-initiating cells (CSC/CIC) as side population (SP) cells. (a) Isolation of SP cells from colon cancer cell lines. SW480, HCT15 and HT29 were stained with Hoechst 33342 dye with or without verapamil and analyzed using a FACSAria II cells sorter. (b) RT-PCR of *DNAJB8*. MP, main population. (c) RT-PCR of CSC/CIC markers in HT29 cells. (d) Tumor growth of HT29 SP cells and MP cells. HT29 SP cells, 10^3, and MP cells were inoculated subcutaneously into the backs of five non-obese diabetic/severe combined immunodeficiency (NOD/SCID) mice and tumor growth was measured weekly. Data represent means ± SD. The difference between SW480 SP and MP cells was examined for statistical significance using the Student's *t*-test.

Discussion

The CSC/CIC are resistant to standard cancer therapies including chemotherapy and radiotherapy,[3] and one of the major topics in research on CSC/CIC is how to target CSC/CIC. Cancer immunotherapy is a novel approach for targeting CSC/CIC. Some reports, including our previous reports, have indicated a relationship between CSC/CIC and immunotherapies. Todaro and colleagues reported that human colon CSC/CIC were killed by γδ T lymphocytes *in vitro*.[28] Ning and colleagues reported that the vaccinations of dendritic cell (DC) pulsed with mice melanoma CSC/CIC and mice squamous cell CSC/CIC conferred effective antitumor effects *in vivo*.[29] However, there have been no reports showing direct killing of human CSC/CIC by CTL. Thus, we analyzed the susceptibility of CRC CSC/CIC specific for CEP55, a novel TAA of CRC.[18] We showed that a CEP55 peptide-specific CTL clone could efficiently recognize SP cells as well as MP cells of human CRC and could kill xenograft tumors derived from SP cells *in vivo*.[18] In the present study, we identified DNAJB8 as a novel CRC CSC/CIC antigen and showed that CTL specific for DNAJB8-derived peptide efficiently recognized SP cells

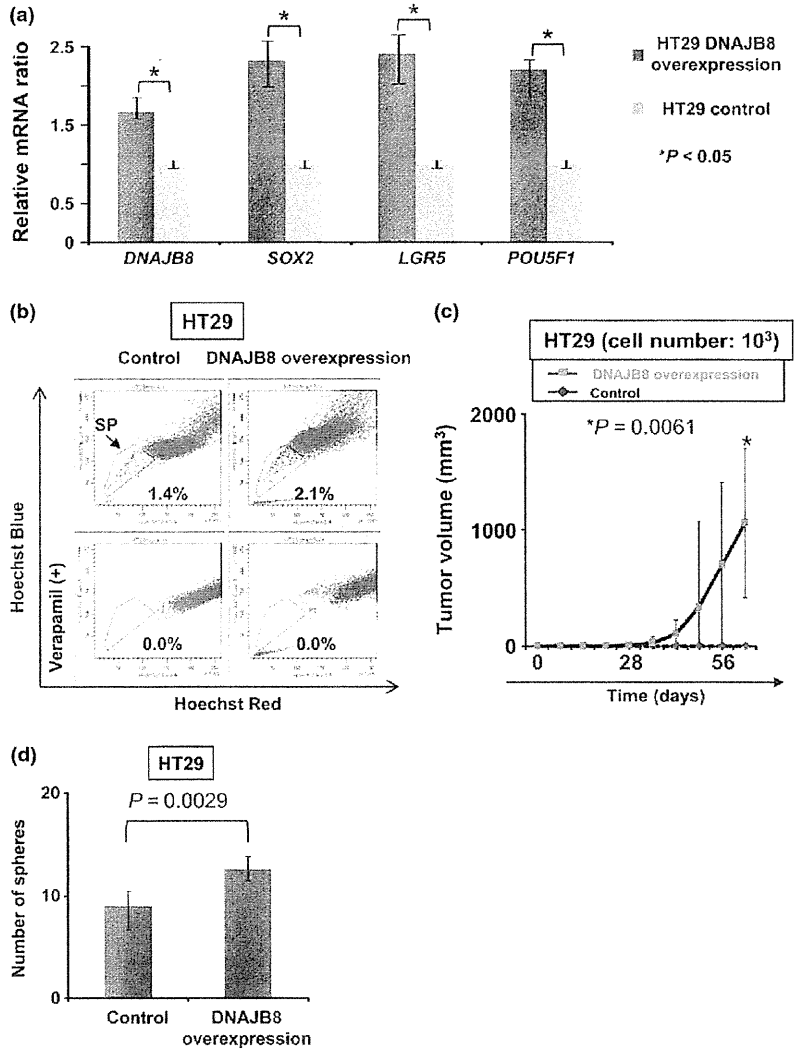

Fig. 2. *DNAJB8* gene overexpression experiments in HT29 cells. (a) Quantitative RT-PCR of *DNAJB8* and colon cancer stem-like cells/cancer-initiating cells (CSC/CIC) markers. Data are shown as a comparison with the expression level in HT29 control cells. Data represent means ± SD. (b) Isolation of side population (SP) cells. HT29 *DNAJB8*-overexpressed cells and control cells were stained with Hoechst 33342 dye with or without verapamil and analyzed using a FACSAria II cell sorter. (c) Tumor growth of HT29 *DNAJB8*-overexpressed cells and control cells. HT29 *DNAJB8*-overexpressed cells, 10^3, and control cells were inoculated subcutaneously into the backs of five non-obese diabetic/severe combined immunodeficiency (NOD/SCID) mice and tumor growth was measured weekly. Data represent means ± SD. The difference between HT29 *DNAJB8*-overexpression cells and control cells was examined for statistical significance using the Student's *t*-test. (d) Sphere formation assay. To assay sphere formation efficiency, 10^3 cells were cultured in Ultra Low Attachment six-well plates for 2 weeks and the number of spheres was counted under a microscope in 15 low-power fields and then the average was calculated.

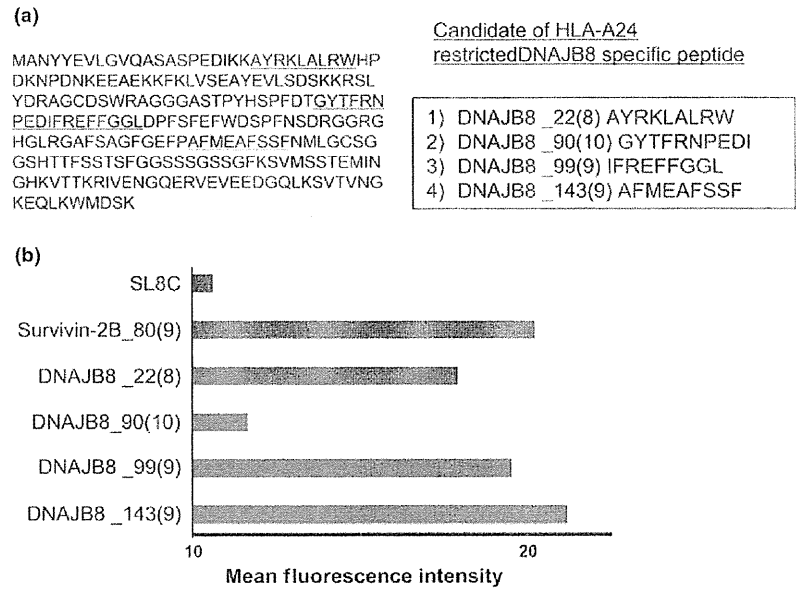

Fig. 3. DNAJB8 peptides carrying a HLA-A24 binding motif. (a) Candidate of DNAJB8 peptides carrying a HLA-A24 binding motif. (b) Peptide-binding assay. Binding affinity was evaluated by comparing mean fluorescence intensity of HLA-A24 expression in the presence of peptide pulsation to mean fluorescence intensity in the absence of the peptide. Survivin-2B_80(9) (AYACNTSTL) peptide was used as a positive control and SL8C (SIINFEKL) peptide was used as a negative control.

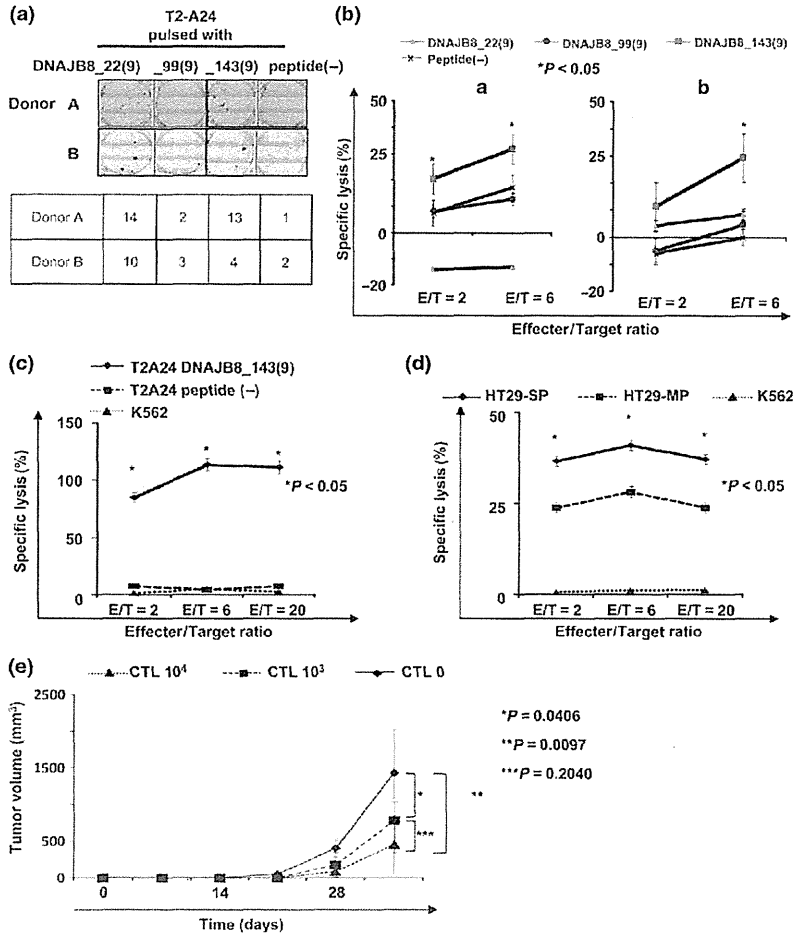

Fig. 4. Antitumor effect of DNAJB8-specific cytotoxic T lymphocyte (CTL) clone. (a) Interferon-γ enzyme-linked immunospot assay. (b) ^{51}Cr release assay. We evaluated specific cytotoxic activity against peptide-pulsed T2-A24 cells in healthy donors. (c, d) ^{51}Cr release assay using the DNAJB8_143(9)-specific CTL clone. We established CTL clones recognizing DNAJB8_143(9) and evaluated cytotoxic activity against side population (SP) cells and main population (MP) cells derived from HT29 cells. (e) Tumor growth of HT29 cells in a therapeutic adoptive transfer model. HT29 cells were inoculated subcutaneously into the back of five NOD/SCID mice and CTL clone cells or PBS was injected intravenously 3 weeks later. Tumor growth was measured weekly. Data represent means ± SD. Differences between groups were examined for statistical significance using the Student's *t*-test.

derived from HT29 cells. The CTL clone specific for CEP55 recognized both SP and MP cells at similar levels,[18] while the CTL clone specific for DNAJB8 recognized SP cells at a higher level than that of MP cells. CEP55 is expressed in both SP and MP cells at similar levels, while DNAJB8 is preferentially expressed in SP cells. Since DNAJB8 is preferentially expressed in CSC/CIC, the combination of DNAJB8-targeting immunotherapy with standard therapies including chemotherapy and radiotherapy might be an effective approach to eradicate cancer. The CTL clone specific for DNAJB8 showed lower, but significant cytotoxicity for MP cells (Fig. 4d), whereas MP cells did not express *DNAJB8* mRNA (Fig. 1b). The SP cells might have the ability to differentiate MP cells and *DNAJB8* mRNA is suppressed according to SP cell differentiation into MP cells. The protein or antigenic peptides of DNAJB8 may remain for a while after differentiation. Therefore, the cytotoxicity for MP cells may be specific for DNAJB8 peptide.

Both the CEP55-specific CTL clone and the DNAJB8-specific CTL clone efficiently recognize CRC CSC/CIC. In our previous review article, we reported that TAA can be distinguished according to the expression patterns in CSC/CIC and non-CSC/CIC, which are: (i) CSC/CIC antigens, which are expressed preferentially in CSC/CIC; (ii) shared antigens, which are expressed in both CSC/CIC and non-CSC/CIC at similar levels; and (iii) non-CSC/CIC antigens, which are preferentially expressed in non-CSC/CIC.[30] In the mouse DNA vaccination model, Dnajb8 showed a greater antitumor effect than that of Survivin.[16] Dnajb8 is a CSC/CIC antigen and Survivin is a shared antigen. CSC/CIC antigens might be better than TAA at achieving an antitumor effect and DNAJB8 might be a better target than CEP55 or Survivin. In our previous clinical trials, we used Survivin-2B-derived antigenic peptides.[7–12] Therefore, use of the CSC/CIC antigen DNAJB8 may therefore improve the clinical outcome of a peptide vaccination trial.

DNAJB8 is a cancer/testis antigen and many other cancer/testis antigens are preferentially expressed in CSC/CIC.[31] However, the functions of most known cancer/testis antigens in CSC/CIC are not known, indicating that there is a risk of antigen loss when targeted by CTL. DNAJB8 has a role in the maintenance of CSC/CIC and it might therefore be a better candidate for CSC/CIC-targeting immunotherapy. In the present study, we used DNAJB8 stably overexpressed cells to analyze the functions of DNAJB8 and most of the cells are supposed to express DNJAB8. However, the increase in rates of SP cells was partial (Fig. 2b). DNAJB8 might be essential for the maintenance of CSC/CIC; however DNAJB8 might not be sufficient and other factor(s) may be necessary to induce CSC/CIC.

In summary, we identified DNAJB8 as a novel functional CSC/CIC antigen in CRC. A DNAJB8-specific CTL clone

derived from a HLA-A*2402 donor showed antitumor ability both *in vitro* and *in vivo*. DNAJB8 is a candidate for CSC/CIC-targeting immunotherapy.

Acknowledgments

The present study was supported by a Grant-in-Aid for Scientific Research from the Ministry of Education, Culture, Sports, Science and Technology of Japan (to N. S.), program for developing the supporting system for upgrading education and research from the Ministry of Education, Culture, Sports, Science and Technology of Japan (to N. S.) and Takeda Science Foundation (to Y. H.) and Research Fellowship of Japan Society for the Promotion of Science for Young Scientists (to R.M.).

Disclosure Statement

The authors have no conflict of interest.

References

1 Markowitz SD, Bertagnolli MM. Molecular origins of cancer: molecular basis of colorectal cancer. *N Engl J Med* 2009; **361**: 2449–60.
2 Clarke MF, Dick JE, Dirks PB *et al.* Cancer stem cells–perspectives on current status and future directions: AACR Workshop on cancer stem cells. *Cancer Res* 2006; **66**: 9339–44.
3 Greaves M, Maley CC. Clonal evolution in cancer. *Nature* 2012; **481**: 306–13.
4 van der Bruggen P, Traversari C, Chomez P *et al.* A gene encoding an antigen recognized by cytolytic T lymphocytes on a human melanoma. *Science* 1991; **254**: 1643–7.
5 Rosenberg SA, Yang JC, Restifo NP. Cancer immunotherapy: moving beyond current vaccines. *Nat Med* 2004; **10**: 909–15.
6 Perez SA, von Hofe E, Kallinteris NL *et al.* A new era in anticancer peptide vaccines. *Cancer* 2010; **116**: 2071–80.
7 Tsuruma T, Hata F, Torigoe T *et al.* Phase I clinical study of anti-apoptosis protein, survivin-derived peptide vaccine therapy for patients with advanced or recurrent colorectal cancer. *J Transl Med* 2004; **2**: 19.
8 Tsuruma T, Iwayama Y, Ohmura T *et al.* Clinical and immunological evaluation of anti-apoptosis protein, survivin-derived peptide vaccine in phase I clinical study for patients with advanced or recurrent breast cancer. *J Transl Med* 2008; **6**: 24.
9 Honma I, Kitamura H, Torigoe T *et al.* Phase I clinical study of anti-apoptosis protein survivin-derived peptide vaccination for patients with advanced or recurrent urothelial cancer. *Cancer Immunol Immunother* 2009; **58**: 1801–7.
10 Kameshima H, Tsuruma T, Torigoe T *et al.* Immunogenic enhancement and clinical effect by type-I interferon of anti-apoptotic protein, survivin-derived peptide vaccine, in advanced colorectal cancer patients. *Cancer Sci* 2011; **102**: 1181–7.
11 Miyazaki A, Kobayashi J, Torigoe T *et al.* Phase I clinical trial of survivin-derived peptide vaccine therapy for patients with advanced or recurrent oral cancer. *Cancer Sci* 2011; **102**: 324–9.
12 Kameshima H, Tsuruma T, Kutomi G *et al.* Immunotherapeutic benefit of IFNalpha in survivin2B-derived peptide vaccination for advanced pancreatic cancer patients. *Cancer Sci* 2013; **104**: 124–9.
13 Hirohashi Y, Torigoe T, Inoda S *et al.* The functioning antigens: beyond just as the immunological targets. *Cancer Sci* 2009; **100**: 798–806.
14 Hageman J, Rujano MA, van Waarde MA *et al.* A DNAJB chaperone subfamily with HDAC-dependent activities suppresses toxic protein aggregation. *Mol Cell* 2010; **37**: 355–69.
15 Sterrenberg JN, Blatch GL, Edkins AL. Human DNAJ in cancer and stem cells. *Cancer Lett* 2011; **312**: 129–42.
16 Nishizawa S, Hirohashi Y, Torigoe T *et al.* HSP DNAJB8 controls tumor-initiating ability in renal cancer stem-like cells. *Cancer Res* 2012; **72**: 2844–54.
17 Goodell MA, Brose K, Paradis G, Conner AS, Mulligan RC. Isolation and functional properties of murine hematopoietic stem cells that are replicating *in vivo*. *J Exp Med* 1996; **183**: 1797–806.
18 Inoda S, Hirohashi Y, Torigoe T *et al.* Cytotoxic T lymphocytes efficiently recognize human colon cancer stem-like cells. *Am J Pathol* 2011; **178**: 1805–13.
19 Nakao M, Shichijo S, Imaizumi T *et al.* Identification of a gene coding for a new squamous cell carcinoma antigen recognized by the CTL. *J Immunol* 2000; **164**: 2565–74.
20 Hirohashi Y, Torigoe T, Maeda A *et al.* An HLA-A24-restricted cytotoxic T lymphocyte epitope of a tumor-associated protein, survivin. *Clin Cancer Res* 2002; **8**: 1731–9.
21 Inoda S, Hirohashi Y, Torigoe T *et al.* Cep55/c10orf3, a tumor antigen derived from a centrosome residing protein in breast carcinoma. *J Immunother* 2009; **32**: 474–85.
22 Haraguchi N, Utsunomiya T, Inoue H *et al.* Characterization of a side population of cancer cells from human gastrointestinal system. *Stem Cells* 2006; **24**: 506–13.
23 Dalerba P, Dylla SJ, Park IK *et al.* Phenotypic characterization of human colorectal cancer stem cells. *Proc Natl Acad Sci USA* 2007; **104**: 10158–63.
24 O'Brien CA, Pollett A, Gallinger S, Dick JE. A human colon cancer cell capable of initiating tumour growth in immunodeficient mice. *Nature* 2007; **445**: 106–10.
25 Ricci-Vitiani L, Lombardi DG, Pilozzi E *et al.* Identification and expansion of human colon-cancer-initiating cells. *Nature* 2007; **445**: 111–5.
26 Huang EH, Hynes MJ, Zhang T *et al.* Aldehyde dehydrogenase 1 is a marker for normal and malignant human colonic stem cells (SC) and tracks SC overpopulation during colon tumorigenesis. *Cancer Res* 2009; **69**: 3382–9.
27 Burkert J, Otto WR, Wright NA. Side populations of gastrointestinal cancers are not enriched in stem cells. *J Pathol* 2008; **214**: 564–73.
28 Todaro M, D'Asaro M, Caccamo N *et al.* Efficient killing of human colon cancer stem cells by gammadelta T lymphocytes. *J Immunol* 2009; **182**: 7287–96.
29 Ning N, Pan Q, Zheng F *et al.* Cancer stem cell vaccination confers significant antitumor immunity. *Cancer Res* 2012; **72**: 1853–64.
30 Hirohashi Y, Torigoe T, Inoda S, Morita R, Kochin V, Sato N. Cytotoxic T lymphocytes: sniping cancer stem cells. *Oncoimmunology* 2012; **1**: 123–5.
31 Yamada R, Takahashi A, Torigoe T *et al.* Preferential expression of cancer/testis genes in cancer stem-like cells: proposal of a novel sub-category, cancer/testis/stem gene. *Tissue Antigens* 2013; **81**: 428–34.